

**SIMPLE QUBIT SYSTEMS
IN BOSONIC BATHS**

NATHAN PUMULO

SIMPLE QUBIT SYSTEMS IN BOSONIC BATHS

NATHAN PUMULO

This dissertation is submitted to the School of Physics, Faculty of Science and Agriculture, University of KwaZulu-Natal, Durban, in fulfillment of the requirements for the degree of Master in Science.

October 2010

As the candidate's supervisor, I have approved this dissertation for submission.

Signed:

Professor Francesco Petruccione

October 2010

The candidate's co-supervisor:

Signed:

Dr. Ilya Sinayskiy

October 2010

Abstract

The study is focused on the thermal entanglement of spin chains. Chains consisting of two and three qubits are considered. These chains are considered open because they are coupled to bosonic baths at different temperatures. The baths represent the environment. The dynamics of these open systems are examined as are the effects of different parameters - such as bath temperature - on the entanglement of the spins. The measure of entanglement used in these cases is the concurrence. Comparisons are made between a model that assumes a strong spin-spin interaction and one that assumes a weak one. In all these cases, analytical solutions for the system dynamics are presented. It is found that at large times, all systems converge to a state that depends only on bath temperature. It is also found that increases in bath temperatures diminish the entanglement between spins and that at high enough temperatures the entanglement vanishes altogether. The time and temperature dependence of the entanglement is different for the two models that are studied.

Publication

The main results of this thesis have been submitted for publication to Journal of Physics A: Mathematical and Theoretical.

Declaration

I declare that the contents of this dissertation are original except where due reference has been made. It has not been submitted before for any degree to any other institution.

Nathan Pumulo

October 2010

Declaration 1 - Plagiarism

I, Nathan Pumulo, declare that

1. The research reported in this thesis, except where otherwise indicated, is my original research.
2. This thesis has not been submitted for any degree or examination at any other university.
3. This thesis does not contain other persons data, pictures, graphs or other information, unless specifically acknowledged as being sourced from other persons.
4. This thesis does not contain other persons' writing, unless specifically acknowledged as being sourced from other researchers. Where other written sources have been quoted, then:
 - a. Their words have been re-written but the general information attributed to them has been referenced
 - b. Where their exact words have been used, then their writing has been placed in italics and inside quotation marks, and referenced.
5. This thesis does not contain text, graphics or tables copied and pasted from the Internet, unless specifically acknowledged, and the source being detailed in the thesis and in the References sections.

Signed:

Acknowledgments

I would like to thank my supervisor Prof. F. Petruccione for affording me the opportunity to come to UKZN to study. Under his supervision my knowledge and appreciation of quantum physics has expanded greatly. I'm grateful for his advice and instruction, and for his sincere concern for my general welfare. I want also to extend special gratitude to the co-supervisor, Dr. I. Sinayskiy. From the beginning to the end, the role he has played in the development of this thesis has been crucial. I will always be indebted to him for his knowledge, his time, his patience with me and his counsel. My studies at UKZN would not have been possible without my sponsors. For the financial support that I received from NITheP, I'm most thankful. Last, but not least, I would like to thank Dr. H. V. Mweene. His academic and moral support both before and during my studies has been invaluable.

Dedication

To my brothers Sinaali and Lutangu
my sister Deborah
my sister-in-law Yolanta
my nephews Lutangu and Ryan
my nieces Sondra-Magdalene and Julie
with love.

Contents

Abstract	ii
Introduction	1
1 Quantum Systems	6
1.1 Closed Quantum Systems	6
1.1.1 The Unitary Time Evolution Operator	6
1.1.2 The Density Operator and its Evolution with Time	7
1.2 Measurement in Quantum Mechanics	9
1.3 Different Pictures In Quantum Mechanics	9
1.4 Open Systems	11
1.5 The Master Equation	14
1.6 Entanglement and Entanglement Measure	16
2 The Strong Spin-Spin Interaction Model	19
2.1 The Model	19
2.2 Strong Spin-Spin Interaction versus Weak Spin-Spin Interaction	21
2.3 The Two-Spin System	23
2.4 The Three-Spin System	30

3	The Weak Spin-Spin Interaction Model	40
3.1	Two Weakly Interacting Spins	42
4	Results	46
4.1	Non-steady State	46
4.2	Steady State	54
5	Conclusion	58
	Appendix: Sets Of Linked Density Matrix Elements	61
	Bibliography	65

Introduction

Up until the beginning of the 20th century, classical physics had been very successful at explaining the physical world. It was assumed at the time that the same laws that correctly described the motion of such macroscopic objects as planets would apply at the microscopic level. So it was quite unexpected when observations began to be made that exposed the limits of the classical approach to physics.

One such observation related to the nature of light. For a long period of time, Huygens' wave theory had been thought to be the correct description of light. Its acceptance over Newton's corpuscular theory had been established by the great success of Maxwell's electrodynamics which interpreted light as electromagnetic waves. Soon enough, however, measurements of the photoelectric effect called into question the correctness of the wave theory of light [1]. One prediction from classical theory regarding the photoelectric effect was that there would be an emission of electrons to the collector at all light frequencies as long as the intensity was sufficiently high. The theory also predicted an increase in the kinetic energy of each electron with increased light intensity. However, it was observed that the kinetic energy of the electrons was dependent only on the frequency of light and not on its intensity. In fact, no electrons were emitted unless the frequency was above a certain threshold level no matter how high the light intensity was.

Another observation that could not be explained classically is blackbody radiation [2]. The view at the time was that light is an electromagnetic wave produced when electric charges vibrate. It was expected that objects with higher temperatures would produce greater vibrations and therefore emit more light. It was assumed that each frequency of vibration had the same energy.

Experiments however showed a very different frequency distribution of the radiant energy.

The study of the hydrogen atom revealed yet more puzzles. In the Rutherford model of the atom, circulating electrons surround the positively charged nucleus. Classically, these electrons are accelerating and are expected to radiate energy and eventually fall into the nucleus [3]. It became clear that a different approach was needed when classical physics failed to explain both the stability and the emission spectrum of even the simplest atom, i.e. hydrogen.

The efforts to find explanations for these and many other observed phenomena led to the development of quantum theory. The difference between classical and quantum mechanics begins with the way the state of any system is described. The consideration of a point system, or a single particle, suffices as an illustration. In classical mechanics, the numerical values of the particle's position and velocity completely specify the state of this system. Thus, if the initial values of these two variables are known, all other dynamical variables related to the system can be found for all times.

The situation in quantum mechanics is rather different. Here, the very act of taking measurement alters the state of the system [1]. This also means that unless they commute, dynamical variables cannot be specified with certainty simultaneously. The system is instead fully described by a state function, i.e. the wave function. The evolution with time of this wave function governs the dynamics of the system.

Quantum mechanics has emerged as a fundamental description for energy and matter at the subatomic level. A central core of the theory is the concept that energy does not take on any value but rather occurs in discrete amounts called quanta. This approach enabled Albert Einstein and Max Planck, respectively, to give explanation for both the photoelectric effect and the Blackbody frequency distribution [4].

Also, unlike in classical physics where waves and particles are separate and distinct, wave-particle duality is an important characteristic of quantum mechanics [1]. This is most evident in experiments involving light. The photoelectric effect shows that light interacts with matter like a particle. The double-slit experiment, on the other hand, reveals that light propagates through space like a wave.

One aspect of quantum mechanics that has no classical equivalence is the concept of entanglement. Entanglement is a quantum mechanical property of two or more objects that are linked in such a way that they cannot be described independently of each other, even if they are spatially separated [5]. The counterintuitive nature of entanglement raises many scientific and philosophical questions. Indeed it had caused even eminent physicists like Albert Einstein to be skeptical about the completeness of the quantum theory [6]. The existence of entanglement, however, has not been in doubt since it was verified experimentally by Alain Aspect in 1982 [7].

The study of entanglement necessarily leads to a fuller appreciation of quantum mechanics and a clearer understanding of how it contrasts with its classical counterpart. Possible applications of entanglement justify its study. Most of the applications of entanglement are best appreciated when compared to and contrasted with schemes that use classical physics.

In recent years, research has been done that shows how quantum computing could possibly allow for the storage of more data and the faster processing of information [8, 9]. The most basic unit of classical information is called a bit. Conventionally, a bit is represented by 1 or 0. An illustration involving a pair of such bits can serve to demonstrate the superiority of quantum information processing over classical information processing. Given a pair of bits, four states are possible, namely 00, 01, 10 and 11. Classically, only one of these possible states can be stored at any one given time in a single register. In quantum mechanics, any two-level system, such as a spin system, can be used as a qubit. The properties of quantum mechanics allow for the storage of all the four possible states at once in a two-qubit quantum register. Because quantum superposition makes it possible to have linear combinations of these states, infinitely more information can be stored. The manipulation and retrieval of information stored in this manner requires an understanding of the entanglement between these qubits and how that is affected by such environmental factors as temperature.

Another field that exploits entanglement is quantum cryptography [10, 11]. Here, entanglement is used to ensure secure communication between two parties. When the entities of an entangled pair are separated, their random but linked properties can be used as a key to encrypt and decrypt information. An important and distinguishing feature of this scheme is that if an

eavesdropper tries to intercept the key, the entanglement breaks and communication stops immediately.

Yet another important application where entanglement plays a direct role is quantum teleportation [12]. This is the quantum process by which information is transmitted from one quantum system to another without transporting the system itself. Indeed, practical demonstration of this phenomenon has been achieved over macroscopic distances [13]. To illustrate what quantum teleportation really is, the following scenario is considered. Suppose Alice holds the part A and Bob the part B of a pair of entangled qubits AB. If Alice and Bob are then separated, the laws of quantum mechanics state that parts A and B will remain entangled. If Alice later wants to send exact information about another qubit C to Bob, it would not be possible for her to do so using classical methods. However, by letting A interact with C, and therefore destroying the entanglement between A and B, Alice can now take measurements on AC that can enable her to transmit two classical bits to Bob who would then have enough information to recreate C exactly. Clearly, an understanding of the phenomenon of entanglement is crucial in the field of quantum teleportation.

One of the challenges faced in trying to realize the applications of quantum mechanics is that when systems are exposed to the environment, they tend to lose their quantum mechanical properties through such processes as decoherence and dissipation [5]. For practical and theoretical reasons, it is important to understand how the dynamics of entangled systems evolve with time when these systems interact with the environment. Over the years much research has been done in the field of thermal entanglement, including notably by [14]. Many studies that have been done in this field have involved the determination of solutions using numerical methods [15]. This thesis focuses on the study of thermal entanglement of spin systems using analytical methods. The spin chains that are studied in this thesis consist of two and three spins. For the two-spins system, each of the spins is coupled to a separate bosonic bath at a different temperature. Two of the three spins in the three-spin system are coupled to separate bosonic baths. The baths represent the environment. Using the concurrence as a measure, the dynamics of the entanglement of these systems is studied in this thesis.

The thesis is laid out as follows. In the first Chapter, closed systems are looked at. These

systems are isolated and have no interaction with any other system. Although they are idealized and do not represent any real systems, the concepts developed in their study are crucial to a broader understanding of quantum mechanics. Two of these concepts, the unitary time evolution operator and the density matrix, are introduced in this Chapter. So too are the different pictures of quantum mechanics. Also discussed in this Chapter are some important elements of the measurement theory in quantum mechanics. Still in the first chapter, an introduction of open quantum systems is presented. The difference between open systems and closed systems is highlighted. Finally, a derivation of the master equation is given, using the Born-Markov approximations.

Two interaction models are studied in this thesis. They are presented in Chapters 2 and 3. The first one, the strong spin-spin interaction model, assumes a strong interaction between the spins. The second, the weak spin-spin interaction model assumes a weak interaction. As will be shown later, this difference in the relative strengths of the interaction results in different energy spectra for the two models. For instance, in the two-spin case, the strong interaction model produces a single spectrum with four different levels, whereas the weak interaction model produces two distinct two-level spectra.

From the equations of motion, the evolution of these systems is analyzed as a function of several parameters such as time and bath temperature. The results and discussion are presented in Chapter 4. The particular property of interest of these systems is entanglement. In order to measure it, the concurrence is used. Chapter 5 is the conclusion.

Chapter 1

Quantum Systems

1.1 Closed Quantum Systems

A quantum state is a mathematical object that contains all the information about a quantum system. In Dirac's bracket notation [16], a pure state is represented by a normalized ket vector $|\psi\rangle$. Closed quantum systems are systems that are assumed to have no interaction with other quantum systems. The evolution with time of these systems can be fully described using unitary dynamics [5]. Although closed quantum systems are idealized and do not represent any real system, their study is important in the development of concepts that can be used to analyze more complicated systems.

1.1.1 The Unitary Time Evolution Operator

The evolution with time of the state of a quantum system is described by the Schrödinger equation

$$i\hbar\frac{\partial}{\partial t}|\psi(t)\rangle = H(t)|\psi(t)\rangle, \quad (1.1)$$

where $|\psi(t)\rangle$ is the state vector, $H(t)$ is the Hamiltonian of the system and \hbar is Planck's constant. In the following we will choose units in such a way that $\hbar = 1$.

The unitary time evolution operator $U(t, t_0)$ transforms the state $|\psi(t_0)\rangle$ at some initial time

t_0 to $|\psi(t)\rangle$ at a later time t . It follows that [5]

$$|\psi(t)\rangle = U(t, t_0)|\psi(t_0)\rangle. \quad (1.2)$$

The initial condition $|\psi(t_0)\rangle$ implies that

$$U(t_0, t_0) = I, \quad (1.3)$$

where I denotes the identity matrix.

Substituting (1.2) into (1.1) and integrating the result yields the expression

$$U(t, t_0) = \exp[-iH(t - t_0)]. \quad (1.4)$$

The unitary nature of this operator means that

$$U^\dagger(t, t_0)U(t, t_0) = U(t, t_0)U^\dagger(t, t_0) = I. \quad (1.5)$$

1.1.2 The Density Operator and its Evolution with Time

In quantum mechanics, the most general states are mixed states. As stated earlier, a pure state can be represented by a single ket $|\psi\rangle$. When an ensemble of pure states is considered, or when the system has been prepared in such a way that it is not certain what pure state it is in, the density matrix is used to represent the system. For a finite dimensional space, it is defined as

$$\rho = \sum_j p_j |\psi_j\rangle\langle\psi_j|, \quad (1.6)$$

where $|\psi_j\rangle$ represent a mixed ensemble of normalized states and the coefficients p_j are corresponding non-negative probability weights that add up to one.

The density matrix has the following properties [5]:

- It is Hermitian,

$$\rho(t) = \rho^\dagger(t).$$

- It has a trace of one

$$\text{Tr}(\rho) = 1.$$

- It is a positive matrix

$$\rho(t) \geq 0.$$

- $\text{Tr}(\rho^2) = 1$ for pure states.
- $\text{Tr}(\rho^2) < 1$ for mixed states.

If the elements of the density operator are denoted by ρ_{nm} , then the diagonal ones ($n = m$) give the probabilities of occupying the quantum states $|\psi_n\rangle$. They are referred to as populations. The off-diagonal ($n \neq m$) elements are complex and have a time-dependent phase factor describing the evolution of coherent superpositions and are referred to as coherences.

From (1.1), (1.2) and (1.5), an expression representing the evolution of the density matrix with time is obtained as outlined below:

$$\begin{aligned}
\frac{d}{dt}\rho(t) &= \frac{d}{dt} \sum_j p_j U(t, t_0) |\psi_j(0)\rangle \langle \psi_j(0)| U^\dagger(t, t_0) \\
&= \sum_j p_j \frac{\partial}{\partial t} U(t, t_0) |\psi_j(0)\rangle \langle \psi_j(0)| U^\dagger(t, t_0) \\
&\quad + \sum_j p_j U(t, t_0) |\psi_j(0)\rangle \langle \psi_j(0)| \frac{\partial}{\partial t} U^\dagger(t, t_0) \\
&= \frac{\partial}{\partial t} U(t, t_0) \rho(0) U^\dagger(t, t_0) + U(t, t_0) \rho(0) \frac{\partial}{\partial t} U^\dagger(t, t_0) \\
&= -iH(t)U(t, t_0)\rho(0)U^\dagger(t, t_0) - iU(t, t_0)\rho(0)U^\dagger(t, t_0)H(t) \\
&= -iH(t)\rho(t) - i\rho(t)H(t).
\end{aligned} \tag{1.7}$$

Hence, using the commutator notation,

$$\frac{d}{dt}\rho(t) = -i[H(t), \rho(t)]. \tag{1.8}$$

This is the Liouville-von Neumann equation. Its formal solution is [5]

$$\rho(t) = U(t, t_0)^\dagger \rho_0 U(t, t_0). \tag{1.9}$$

1.2 Measurement in Quantum Mechanics

We consider a quantum mechanical system described by the wave function $|\psi(t)\rangle$. One of the postulates of quantum mechanics states that associated with each measurement on the system is a Hermitian operator A called an observable. The only possible result of a measurement of the observable is one of the eigenvalues of A . The fact that A is Hermitian means that all its eigenvalues are real. If the observable A has a discrete spectrum, the results of the measurements are quantized [2]. If, in addition to having a discrete spectrum, the eigenvalues a_n of the observable A are non-degenerate, then there is, corresponding to each of them, a unique eigenvector $|\phi_n(t)\rangle$. Therefore, the eigenvalue equation for the operator can be written

$$A|\phi_n\rangle = a_n|\phi_n\rangle. \quad (1.10)$$

Using the principle of superposition, the normalized eigenvectors $|\phi_n(t)\rangle$ can be used to write the wave function as [1]:

$$|\psi(t)\rangle = \sum_n c_n |\phi_n(t)\rangle, \quad (1.11)$$

where c_n are expansion coefficients which in general are complex functions of time. The probability $P(a_n)$ of obtaining a_n when A is measured is

$$P(a_n) = |c_n|^2 \quad (1.12)$$

and the expectation value of A is

$$\langle A \rangle = \sum_n |c_n|^2 a_n. \quad (1.13)$$

1.3 Different Pictures In Quantum Mechanics

An important aspect of representation in quantum mechanics involves the different pictures of the theory. These pictures represent alternative but equivalent formulations of the theory. The eigenvalues of operators corresponding to observables are the same, and the inner products of state vectors maintain their values as well [3]. The difference in the pictures lies in the way time evolution is treated.

In the Schrödinger picture description of the dynamical evolution of quantum systems, the state vectors $|\psi(t)\rangle$ are time-dependent. The physical quantities are described by time-independent operators. In the Heisenberg picture, the state vectors are time-independent and the dynamical evolution of the system is described by time-dependent operators [1]. Transitions between the Schrödinger picture and the Heisenberg picture is accomplished through a unitary time-dependent transformation.

If A_H is an operator in the Heisenberg picture and A_S is an operator in the Schrödinger picture, then [5]

$$A_H(t) = U^\dagger(t, t_0)A_S U(t, t_0), \quad (1.14)$$

where $U(t, t_0)$ is the unitary time evolution operator given by (1.4).

The variation of A_H with time is defined as

$$\frac{d}{dt}A_H(t) = \frac{\partial}{\partial t}U A_S U^\dagger + U \frac{\partial}{\partial t}A_S U^\dagger + U A_S \frac{\partial}{\partial t}U^\dagger. \quad (1.15)$$

From the Schrödinger equation

$$i \frac{\partial}{\partial t}U(t, t_0) = H U(t, t_0)$$

and the hermiticity of the Hamiltonian

$$H = H^\dagger,$$

it follows from (1.15) that

$$\frac{d}{dt}A_H(t) = -i(U H A_S U^\dagger - U A_S H U^\dagger) + U \frac{\partial}{\partial t}A_S U^\dagger. \quad (1.16)$$

Therefore, the evolution with time of a Heisenberg operator is concisely written in commutator notation as

$$\frac{d}{dt}A_H(t) = -iU[H, A_S]U^\dagger + U \frac{\partial}{\partial t}A_S U^\dagger. \quad (1.17)$$

A representation that is more general than both the Heisenberg picture and the Schrödinger picture is the interaction picture. In this representation the Hamiltonian of a quantum system can be written as a sum of two parts

$$H_S = H_O + H_I, \quad (1.18)$$

where H_O is time-independent and H_I is the interaction energy operator of the system. The exact nature of the division of the Hamiltonian depends on the situation being studied.

Transition from the interaction picture to other pictures is done through unitary transformations. Thus a state vector in the interaction picture is defined by

$$|\psi_I(t)\rangle = U_O^\dagger(t, t_0)|\psi_S(t)\rangle, \quad (1.19)$$

where $\psi_S(t)$ is the same state vector in the Schrödinger picture.

The interaction picture density matrix $\rho_I(t)$ and the Schrödinger picture density matrix $\rho(t)$ are connected through the transformation

$$\rho_I(t) = U_I^\dagger(t, t_0)\rho(t)U_I(t, t_0), \quad (1.20)$$

where

$$U_I(t, t_0) = U_O^\dagger(t, t_0)U(t, t_0), \quad (1.21)$$

$$U_O(t, t_0) = \exp[-i(t - t_0)H_O] \quad (1.22)$$

and

$$U(t, t_0) = \exp[-i(t - t_0)(H_O + H_I)] = \exp[-i(t - t_0)H_S]. \quad (1.23)$$

The time evolution of the interaction picture density matrix is given by the Liouville-von Neumann equation as

$$\frac{d}{dt}\rho_I(t) = -i[H_I(t), \rho_I(t)]. \quad (1.24)$$

In the interaction picture representation, emphasis is put on the interaction Hamiltonian. The interaction picture is best applied in situations where a small interaction term is considered in addition to the Hamiltonian of a solved system. This is the case in open quantum systems which are introduced in the next section.

1.4 Open Systems

Until fairly recently, most studies in quantum mechanics had involved closed quantum systems. Closed quantum systems are assumed to be isolated. There is, therefore, no interchange of

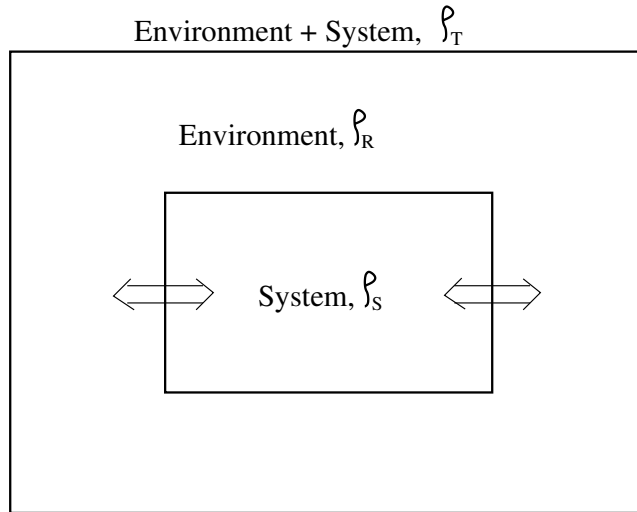


Figure 1.1: A schematic representation of an open quantum system.

energy and entropy between these systems and any other system. The evolution with time of closed quantum systems is sufficiently described by unitary dynamics.

The need for an approach that more closely describes real-life quantum systems has led to more research in the field of open quantum systems. The realization of most applications of quantum mechanics would not be possible without a clear understanding of open quantum system dynamics. For instance, dissipation and decoherence are just two of the phenomena that inevitably have to be dealt with in any such application.

Open system dynamics are exhaustively looked at in [5], and it is from there that the following description is largely drawn. If a quantum system S is coupled to a larger system R , S is said to be an open quantum system. The larger system is generally taken to be the environment or reservoir. This is shown schematically in Figure 1.1. The dynamics of the system will be more complicated than in a closed system case. This means there is now an interchange of energy and entropy between the system and the environment. The interaction results in system-reservoir correlations such that unitary dynamics can no longer represent the state changes in the subsystem. The subsystem S is now called the reduced system and the effects on it brought about by the total system define the reduced system dynamics. The evolution of the reduced system S now becomes a function of both its internal dynamics and its interaction with the environment. The term bath is used to refer to an environment with an infinite number of

degrees of freedom and in a thermal equilibrium state.

If \mathcal{H}_S is the Hilbert space for the sub-system, and \mathcal{H}_R that for the environment, the Hilbert space for the combined system is the tensor product $\mathcal{H}_S \otimes \mathcal{H}_R$. The total Hamiltonian is

$$H = H_S + H_R + H_I, \quad (1.25)$$

where H_S is the Hamiltonian for the reduced system. H_R is the Hamiltonian for the environment, and H_I is the interaction Hamiltonian. A complete study of the dynamics of the combined system is very difficult to accomplish. As an example, if the environment is a heat bath, a complete study would require the solution of an infinite number of coupled equations of motion. However, the system S can be studied without having a complete knowledge of R .

The evolution with time of an open quantum system is best described by a dynamical map. If it is assumed that the initial state of the combined system (open system + environment) ρ_T is given by

$$\rho_T(0) = \rho_S(0) \otimes \rho_R, \quad (1.26)$$

where $\rho_S(0)$ is the initial state of the open system and ρ_R that of the environment, then the transformation that connects the initial state $\rho_S(0)$ at $t = 0$ to the final state $\rho_S(t)$ at $t > 0$ can be written as [5]

$$\rho_S(0) \mapsto \rho_S(t) = V(t)\rho_S(0) \equiv \text{Tr}_R\{U(t,0)[\rho_S(0) \otimes \rho_R]U^\dagger(t,0)\}. \quad (1.27)$$

In the above expression, Tr_R denotes the trace taken over the degrees of freedom of the environment R and $V(t)$ is the dynamical map. $V(t)$ is a genuine quantum operation which meets the following criteria:

- It is trace preserving.
- It is convex-linear.
- It is completely positive.

It has been shown in [5] how the above axioms, when combined with the Markov assumption, make it possible to represent the time evolution of the open system in the Schrödinger picture

by the master equation

$$\frac{d}{dt}\rho_S = -i[H_S, \rho_S] + \sum_{k=1}^N \gamma_k (A_k \rho_S A_k^\dagger - \frac{1}{2} A_k^\dagger A_k \rho_S - \frac{1}{2} \rho_S A_k A_k^\dagger). \quad (1.28)$$

The first term on the right hand side of (1.28) represents the unitary evolution of the system due to the Hamiltonian H_S . The second term, which is also called the dissipator $D(\rho)$, is a direct result of the coupling with the environment. The dimension of the state space is characterized by N . The operators A_k and A_k^\dagger are linear combinations of basis operators. In a two-dimensional space, for example, these basis operators would be the Pauli matrices. Correlation functions in the environment are represented by γ_k .

1.5 The Master Equation

The dynamics of closed quantum systems are represented in terms of a unitary time evolution. This cannot be done with open quantum systems. Equations of motion for the density matrix are instead used to represent the dynamics of open systems. These are the master equations for these systems [5].

In order for the time evolution of the density matrix of an open quantum system to be defined by (1.28), some important assumptions and approximations have to be made. In the following, a master equation representing the time evolution of the reduced system S that is coupled to the environment R is derived. The approach used is based on the presentation by [5],[17] and [18].

The Hamiltonian of the combined system is given by (1.25). The density operator ρ_S for the reduced system is defined by

$$\rho_S = \text{Tr}_R[\rho_T(t)], \quad (1.29)$$

where ρ_T is the density operator of the combined system and Tr_R denotes the partial trace which is taken over the degrees of freedom of R .

Knowledge of ρ_S alone is sufficient for calculations of expectation values of operators in S to

be made. If A is an operator acting on \mathcal{H}_S , then

$$\langle A \rangle = \text{Tr}_S[A\rho_S], \quad (1.30)$$

where Tr_S denotes the partial trace over the Hilbert space of the reduced system S .

The derivation of the master equation is best done in the interaction picture. In this picture, the Liouville-von Neumann equation (1.8) becomes

$$\frac{d}{dt}\tilde{\rho}_T = -i[\tilde{H}_I(t), \tilde{\rho}_T], \quad (1.31)$$

where $\tilde{H}_I(t)$ and $\tilde{\rho}_T$ respectively are representations of the interaction Hamiltonian and the density matrix in the interaction picture and are given by

$$\tilde{H}_I = e^{i(H_S+H_R)t} H_I e^{-i(H_S+H_R)t} \quad (1.32)$$

and

$$\tilde{\rho}_T = e^{i(H_S+H_R)t} \rho_T e^{-i(H_S+H_R)t}. \quad (1.33)$$

It is assumed that no correlations exist between the system and the bath at $t = 0$. This means that the density operator factorizes

$$\rho_T(0) = \tilde{\rho}_T(0) \approx \rho_S(0) \otimes \rho_R. \quad (1.34)$$

Equation (1.31) is integrated from 0 to t . Given the condition (1.34), after two iterations, we get

$$\tilde{\rho}_T(t) = \tilde{\rho}_T(0) - i \int_0^t dt' [\tilde{H}_I(t'), \tilde{\rho}_T(0)] - \int_0^t dt' \int_0^{t'} dt'' [\tilde{H}_I(t'), [\tilde{H}_I(t''), \tilde{\rho}_T(t'')]]. \quad (1.35)$$

Differentiation of (1.35) yields an integro-differential equation for $\tilde{\rho}_T$

$$\frac{d}{dt}\tilde{\rho}_T = -i[\tilde{H}_I(t), \tilde{\rho}_T(0)] - \int_0^t dt' [\tilde{H}_I(t), [\tilde{H}_I(t'), \tilde{\rho}_T(t')]]. \quad (1.36)$$

At $t > 0$, correlations develop between the system and the reservoir. Two important approximations are made at this point. The first, the Born approximation, assumes that this coupling is very weak. H_I is much less than H_R and H_S and that the interaction has little effect on the

reservoir density operator. Thus at any time t the density operator can be written as the direct product

$$\tilde{\rho}_T(t) \approx \rho_S(t) \otimes \rho_R. \quad (1.37)$$

The trace can now be taken over the reservoir states. Taking note of (1.29) and the assumption that the first term on the right side of (1.36) vanishes

$$\text{Tr}_R[\tilde{H}_I(t), \rho_R] = 0,$$

it can now be seen that

$$\frac{d}{dt}\tilde{\rho}_S = - \int_0^t dt' \text{Tr}_R[\tilde{H}_I(t), [\tilde{H}_I(t'), \tilde{\rho}_S(t') \otimes \rho_R]]. \quad (1.38)$$

The second simplification is the Markovian approximation. The presence of $\rho_S(t')$ in (1.38) means that the evolution of the system depends on its history. If it is assumed that the bath is a large system, it is not expected that the small changes brought about by its interaction with the much smaller subsystem S will have an impact on it that will affect the future evolution of S . This means that in the integrand $\rho_S(t')$ can now be replaced by $\rho_S(t)$. In the integration above, t' represents the decay of reservoir correlations. It is a much shorter time than the time scale for changes in $\tilde{\rho}_S$. Therefore, the upper limit in the integral can be extended to infinity. Thus, (1.38) becomes

$$\frac{d}{dt}\tilde{\rho}_S = - \int_0^\infty dt' \text{Tr}_R[\tilde{H}_I(t), [\tilde{H}_I(t'), \tilde{\rho}_S(t) \otimes \tilde{\rho}_R]]. \quad (1.39)$$

This is the master-equation in the Born-Markov approximation.

In the next chapter Eq. (1.39) will be used and put in the form of (1.28) to give the evolution with time of two and three-spin systems which are coupled to the environment.

1.6 Entanglement and Entanglement Measure

A central theme of this thesis is the study of the evolution with time of entangled spin systems. It is thus imperative to give a mathematical description of entangled states. A concise definition of entanglement is given in [5].

The following suffices as a description of an entangled system. Two interacting systems S_A and S_B with respective Hilbert spaces \mathcal{H}_A and \mathcal{H}_B are considered. The Hilbert space of the combined system $S = S_A + S_B$ is the tensor product of the two subsystems S_A and S_B

$$\mathcal{H} = \mathcal{H}_A \otimes \mathcal{H}_B. \quad (1.40)$$

If $|\psi\rangle_A$ is a state of the system S_A and $|\psi\rangle_B$ that of the system S_B , then a state

$$|\psi\rangle \in \mathcal{H}_A \otimes \mathcal{H}_B. \quad (1.41)$$

is said to be entangled if it cannot be written as a tensor product $|\psi_A\rangle \otimes |\psi_B\rangle$. If it can be written as a tensor product of the states of the subsystems, it is said to be separable.

In this research, we study the dynamics of the entanglement between the qubits. For a successful analysis, a good measure of entanglement is required. One such measure is the negativity. It is based on the fact that if a state is separable the partial transpose of its density matrix is a valid state that is positive semidefinite [19]. This is not the case for entangled states as their partial transpose may have one or more negative eigenvalues. The degree to which a state does not obey the positive partial transpose *PPT* separability criterion can, therefore, be used as an indicator of the negativity of the state [20] and, by extension, its entanglement. One well used definition of the negativity $N(\rho)$ is [21]

$$N(\rho) \equiv \frac{\|\rho^{TA}\| - 1}{2}, \quad (1.42)$$

where $\|\rho^{TA}\|$ denotes the trace norm of the partial transpose ρ^{TA} of the density matrix ρ . The expression (1.40) corresponds to the sum of the absolute values of the eigenvalues of ρ^{TA} . For unentangled states, this quantity vanishes.

In this thesis, a different measure of entanglement is used. This is the concurrence, $C(\rho)$. For a two-qubit system, it is defined as [22]

$$C(\rho) = \max\{0, \sqrt{\lambda_1} - \sqrt{\lambda_2} - \sqrt{\lambda_3} - \sqrt{\lambda_4}\}. \quad (1.43)$$

The λ_i are the eigenvalues of a matrix R which is defined as

$$R = \sqrt{\sqrt{\rho}(\sigma_y \otimes \sigma_y)\sqrt{\rho}(\sigma_y \otimes \sigma_y)}. \quad (1.44)$$

The eigenvalues λ_i are ordered in such a way that $\lambda_1 \geq \lambda_2 \geq \lambda_3 \geq \lambda_4$. For computational purposes, the same results are obtained when the matrix R is defined as

$$R = \rho(\sigma_y \otimes \sigma_y) \rho^*(\sigma_y \otimes \sigma_y). \quad (1.45)$$

In both cases ρ is the density matrix of the system, ρ^* is its complex conjugate and

$$\sigma_y = \begin{pmatrix} 0 & -i \\ i & 0 \end{pmatrix}$$

is a Pauli matrix.

Chapter 2

The Strong Spin-Spin Interaction Model

2.1 The Model

In this thesis, systems consisting of two and three spins are considered. These spins are coupled to two separate bosonic baths at different temperatures. In the scheme used here, each bath represents a reservoir of harmonic oscillators with frequencies $\omega_{n,j}$, and creation and annihilation operators $b_{n,j}$ and $b_{n,j}^\dagger$. Here, the index j represents each of the baths and n indicates the reservoir modes. The equilibrium state of the baths ρ_R is taken to be [5]

$$\rho_R = \frac{\exp(-H_S/k_B T)}{\text{Tr}[\exp(-H_S/k_B T)]}, \quad (2.1)$$

where H_S is the system Hamiltonian, T is the bath temperature and k_B is the Boltzmann constant which in the following is set equal to 1.

The model is shown schematically in Figure 2.1. The total Hamiltonian for the system is given by [5]

$$H = H_S + H_{Bj} + H_I, \quad (2.2)$$

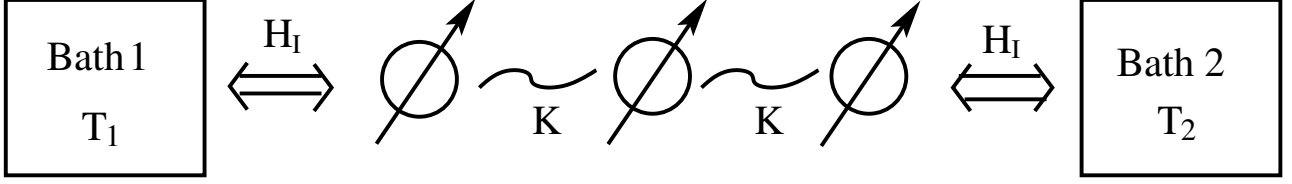


Figure 2.1: A schematic picture of the model under study. A three-spin system is coupled to two separate baths at temperatures T_1 and T_2 . H_I is the system-bath interaction Hamiltonian. K denotes the strength of the spin-spin interaction.

where the Hamiltonian H_S is

$$\hat{H}_S = \sum_i^N \frac{\epsilon_i}{2} \sigma_i^z + K \sum_i^{N-1} (\sigma_i^+ \sigma_{i+1}^- + \sigma_i^- \sigma_{i+1}^+). \quad (2.3)$$

In the above expression N denotes the number of spins of the system, the ϵ_i denote the energies of the spins and the constant K denotes the strength of the spin-spin interaction. The operators σ_i^z and σ_i^\pm are the Pauli matrices of the subsystem.

H_{Bj} is the Hamiltonian of the bosonic baths. For each bath j , the Hamiltonian is given by [23]

$$H_{Bj} = \sum_n \omega_{n,j} b_{n,j}^\dagger b_{n,j}. \quad (2.4)$$

H_I is the Hamiltonian of the interaction between each bath and the subsystem and is given by

$$\hat{H}_I = \sum_{j,n} g_n b_{j,n}^\dagger \sigma_j^- + \sum_{j,n} g_n^* b_{j,n} \sigma_j^+, \quad (2.5)$$

where g_n and g_n^* are coupling constants. It is assumed that the Hamiltonian of the interaction can be represented in the form [23]

$$H_I = \sum_{j,i} (f_{j,i} V_{j,i}^\dagger + f_{j,i}^\dagger V_{j,i}), \quad (2.6)$$

where $f_{j,i}$ and $f_{j,i}^\dagger$ act on the Hilbert space of the bath. $V_{j,i}^\dagger$ and $V_{j,i}$ act on the Hilbert space of the system and are, therefore, eigenoperators of the system Hamiltonian H_S . These operators are chosen in such a way that

$$[H_S, V_{j,i}] \equiv -\omega_{j,i} V_{j,i} \quad (2.7)$$

and

$$[H_S, V_{j,i}^\dagger] \equiv \omega_{j,i} V_{j,i}^\dagger, \quad (2.8)$$

where $\omega_{j,i}$ are the frequencies of the transitions.

The above equations are general and can be applied to systems with any number of spins. Depending on the strength of interaction between the spins, two different models are obtained. The difference between these models is explained in the section that follows.

2.2 Strong Spin-Spin Interaction versus Weak Spin-Spin Interaction

In this thesis, two models are studied: the strong spin-spin interaction model and the weak spin-spin interaction model. It is emphasized here that the interaction between the spins and the environment is always considered weak. It is this assumption that has allowed for the derivation of the master equation in the Born-Markov approximation. The model names used refer to the relative strengths of interaction between the spins themselves. The information on the frequencies of the bath modes and their coupling to the spin systems is contained in a function called the spectral density $J(\omega)$. If the master equation (1.28) is used as an example for this case, the spectral density would be in the environmental correlation functions γ_k . In the models that are presented, $J(\omega)d\omega$ gives the number of oscillators with frequencies in the interval ω to $\omega + d\omega$. The particular one used in this thesis is the Lorentzian distribution [5]

$$J(\omega) = \frac{\gamma}{2\pi} \frac{\Gamma^2}{(\omega_o - \omega)^2 + \Gamma^2}, \quad (2.9)$$

where ω is the frequency of the bath modes and ω_o is the transition frequency of the spin system. The parameter Γ is such that Γ^{-1} is equal to the reservoir correlation time and defines the spectral width of the coupling. γ^{-1} is equal to the time scale on which the system changes.

In the strong spin-spin interaction model, the condition that $\epsilon \sim K \gg \gamma$ holds. In the weak spin-spin interaction model, $\epsilon \gg K \sim \gamma$. The strength of the spin-spin interaction is denoted by K .

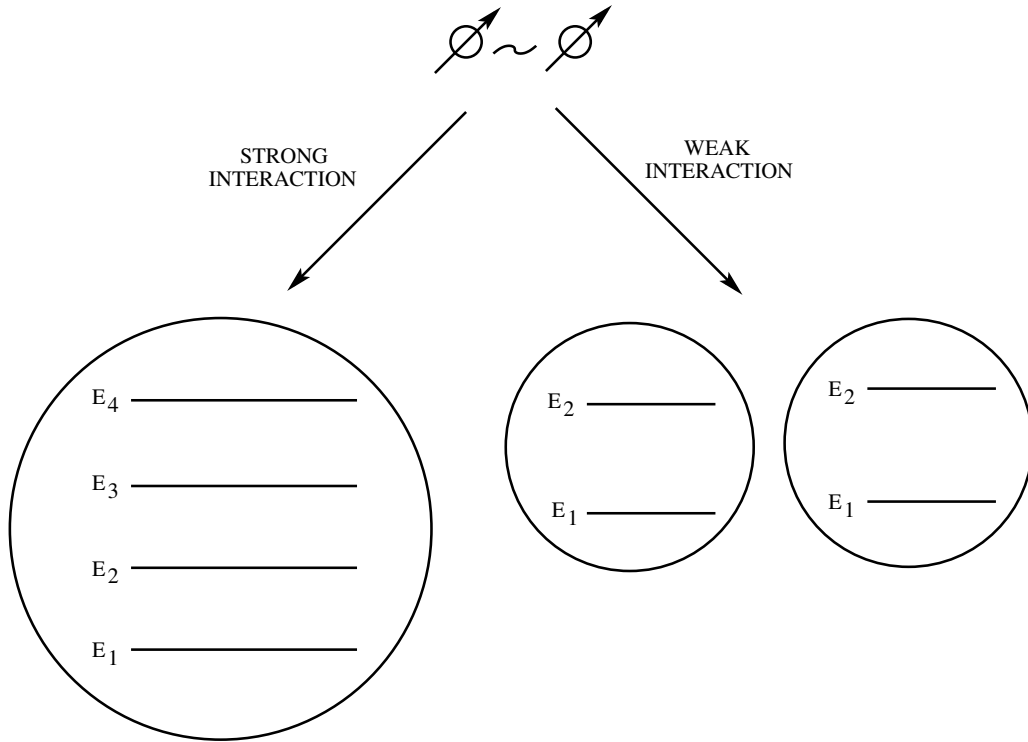


Figure 2.2: A schematic picture showing the energy spectra of two two-level systems. The shape of the resulting energy spectrum depends on which model is considered; the strong spin-spin interaction model or the weak spin-spin interaction model.

The result of this difference is seen in the structure of the systems formed by the interaction, i.e. the energy spectra. For example, in the two-spin case, the strong spin-spin interaction results in the formation of a single system with four different energy levels. Although there is interaction between the two spins in the weak spin-spin interaction model, in their interaction with the environment, they can be treated as two separate systems. This is the case even for higher spin systems. Generally, an n -spin case results in a single system with n^2 energy levels in the strong interaction model. In the weak interaction model, two distinct sets of n energy levels are formed. This is shown diagrammatically in Fig. 2.2 for the two-spin system.

2.3 The Two-Spin System

An integrable or exactly solvable model is considered for the strong two-spin system. It is demonstrated below how the equation of motion (1.28) for the density operator can be obtained for the two-spin system. A similar treatment for higher spin systems yields equivalent results.

The environment consists of two bosonic baths. Each spin of the sub-system is coupled to a separate bath. The interaction between each bath and the subsystem S is given by (2.5).

In this particular model, strong spin-spin interaction means that instead of two distinct two-level systems, a single four-level system is formed. In the interaction picture, the interaction picture Hamiltonian (2.5) can be written as

$$H_I(t) = \sum_{j,i} (f_{j,i} V_{j,i}^\dagger e^{i\omega_{j,i}t} + f_{j,i}^\dagger V_{j,i} e^{-i\omega_{j,i}t}). \quad (2.10)$$

The index i represents the transition levels and j indicates the bath. This means that for a two-spin system, the master equation (1.39) becomes

$$\begin{aligned} \frac{d}{dt} \tilde{\rho} = - \int_0^\infty dt' \text{Tr}_R \sum_{n,j} \sum_{m,k} [g_{n,j} \hat{b}_{n,j}^\dagger e^{i\omega_{n,j}t} (V_{j,1} e^{-i\omega_1 t} + V_{j,2} e^{-i\omega_2 t}) + g_{n,j}^* \hat{b}_{n,j} e^{-i\omega_{n,j}t} (V_{j,1}^\dagger e^{i\omega_1 t} + V_{j,2}^\dagger e^{i\omega_2 t}), \\ [g_{m,k} \hat{b}_{m,k}^\dagger e^{i\omega_{m,k}t'} (V_{k,1} e^{-i\omega_1 t'} + V_{k,2} e^{-i\omega_2 t'}) + g_{m,k}^* \hat{b}_{m,k} e^{-i\omega_{m,k}t'} (V_{k,1}^\dagger e^{i\omega_1 t'} + V_{k,2}^\dagger e^{i\omega_2 t'})], \rho(t) \otimes \rho_R]. \end{aligned} \quad (2.11)$$

Here, the indices m and k correspond to n and j respectively, and are introduced in order to make a distinction between the two Hamiltonians of the commutator in (1.39). For convenience, the index S in $\rho_S(t)$ has been dropped.

The trace is now taken over the Hilbert space of the reservoir. For the canonical bosonic reservoir considered, the following statements hold [17]:

$$\text{Tr}_R \{ \hat{b}_{n,j} \hat{b}_{m,k} \rho_R \} = 0; \quad (2.12)$$

$$\text{Tr}_R \{ \hat{b}_{n,j}^\dagger \hat{b}_{m,k}^\dagger \rho_R \} = 0; \quad (2.13)$$

$$\text{Tr}_R \{ \hat{b}_{n,j} \hat{b}_{m,k}^\dagger \rho_R \} = (n(\omega_{n,j}, T_j) + 1) \delta_{m,n} \delta_{k,j}; \quad (2.14)$$

$$\text{Tr}_R \{ \hat{b}_{n,j}^\dagger \hat{b}_{m,k} \rho_R \} = n(\omega_{n,j}, T_j) \delta_{m,n} \delta_{k,j}, \quad (2.15)$$

where

$$n(\omega_{n,j}, T_j) = \frac{1}{\exp(\frac{\omega_{n,j}}{T_j}) - 1}$$

is the mean photon number for an oscillator with frequency $\omega_{n,j}$ in thermal equilibrium at temperature T .

Multiplying out the terms and introducing τ such that $t' = t - \tau$, (2.11) can now be written as

$$\begin{aligned} \frac{d}{dt} \bar{\rho} = & - \sum_{n,j} \int_0^t d\tau [V_{j,1} V_{j,1}^\dagger \rho(t) e^{-i(\omega_1 - \omega_{n,j})\tau} |g_{n,j}|^2 n(\omega_{n,j}, T_j) + V_{j,1} V_{j,2}^\dagger \rho(t) e^{-i(\omega_1 - \omega_2)t - i(\omega_2 - \omega_{n,j})\tau} |g_{n,j}|^2 n(\omega_{n,j}, T_j) \\ & + V_{j,2} V_{j,2}^\dagger \rho(t) e^{-i(\omega_2 - \omega_{n,j})\tau} |g_{n,j}|^2 n(\omega_{n,j}, T_j) + V_{j,2} V_{j,1}^\dagger \rho(t) e^{-i(\omega_2 - \omega_1)t - i(\omega_1 - \omega_{n,j})\tau} |g_{n,j}|^2 n(\omega_{n,j}, T_j) \\ & - V_{j,1}^\dagger \rho(t) V_{j,1} e^{-i(\omega_1 - \omega_{n,j})\tau} |g_{n,j}|^2 n(\omega_{n,j}, T_j) - V_{j,1}^\dagger \rho(t) V_{j,2} e^{-i(\omega_2 - \omega_1)t - i(\omega_1 - \omega_{n,j})\tau} |g_{n,j}|^2 n(\omega_{n,j}, T_j) \\ & - V_{j,2}^\dagger \rho(t) V_{j,2} e^{-i(\omega_2 - \omega_{n,j})\tau} |g_{n,j}|^2 n(\omega_{n,j}, T_j) - V_{j,2}^\dagger \rho(t) V_{j,1} e^{-i(\omega_1 - \omega_2)t - i(\omega_2 - \omega_{n,j})\tau} |g_{n,j}|^2 n(\omega_{n,j}, T_j) \\ & + \rho(t) V_{j,1}^\dagger V_{j,1} e^{-i(\omega_1 - \omega_{n,j})\tau} |g_{n,j}|^2 (n(\omega_{n,j}, T_j) + 1) + \rho(t) V_{j,1}^\dagger V_{j,2} e^{-i(\omega_2 - \omega_1)t - i(\omega_1 - \omega_{n,j})\tau} |g_{n,j}|^2 (n(\omega_{n,j}, T_j) + 1) \\ & + \rho(t) V_{j,2}^\dagger V_{j,1} e^{-i(\omega_2 - \omega_{n,j})\tau} |g_{n,j}|^2 (n(\omega_{n,j}, T_j) + 1) + \rho(t) V_{j,2}^\dagger V_{j,2} e^{-i(\omega_1 - \omega_2)t - i(\omega_2 - \omega_{n,j})\tau} |g_{n,j}|^2 (n(\omega_{n,j}, T_j) + 1) \\ & - V_{j,1} \rho(t) V_{j,1}^\dagger e^{-i(\omega_1 - \omega_{n,j})\tau} |g_{n,j}|^2 (n(\omega_{n,j}, T_j) + 1) - V_{j,1} \rho(t) V_{j,2}^\dagger e^{-i(\omega_1 - \omega_2)t - i(\omega_2 - \omega_{n,j})\tau} |g_{n,j}|^2 (n(\omega_{n,j}, T_j) + 1) \\ & - V_{j,2} \rho(t) V_{j,2}^\dagger e^{-i(\omega_2 - \omega_{n,j})\tau} |g_{n,j}|^2 (n(\omega_{n,j}, T_j) + 1) - V_{j,2} \rho(t) V_{j,1}^\dagger e^{-i(\omega_2 - \omega_1)t - i(\omega_1 - \omega_{n,j})\tau} |g_{n,j}|^2 (n(\omega_{n,j}, T_j) + 1) \\ & + V_{j,1}^\dagger V_{j,1} \rho(t) e^{i(\omega_1 - \omega_{n,j})\tau} |g_{n,j}|^2 (n(\omega_{n,j}, T_j) + 1) + V_{j,1}^\dagger V_{j,2} \rho(t) e^{-i(\omega_2 - \omega_1)t + i(\omega_2 - \omega_{n,j})\tau} |g_{n,j}|^2 (n(\omega_{n,j}, T_j) + 1) \\ & + V_{j,2}^\dagger V_{j,2} \rho(t) e^{i(\omega_2 - \omega_{n,j})\tau} |g_{n,j}|^2 (n(\omega_{n,j}, T_j) + 1) + V_{j,2}^\dagger V_{j,1} \rho(t) e^{-i(\omega_1 - \omega_2)t + i(\omega_1 - \omega_{n,j})\tau} |g_{n,j}|^2 (n(\omega_{n,j}, T_j) + 1) \\ & - V_{j,1} \rho(t) V_{j,1}^\dagger e^{i(\omega_1 - \omega_{n,j})\tau} |g_{n,j}|^2 (n(\omega_{n,j}, T_j) + 1) - V_{j,1} \rho(t) V_{j,2}^\dagger e^{-i(\omega_1 - \omega_2)t + i(\omega_1 - \omega_{n,j})\tau} |g_{n,j}|^2 (n(\omega_{n,j}, T_j) + 1) \\ & - V_{j,2} \rho(t) V_{j,2}^\dagger e^{i(\omega_2 - \omega_{n,j})\tau} |g_{n,j}|^2 (n(\omega_{n,j}, T_j) + 1) - V_{j,2} \rho(t) V_{j,1}^\dagger e^{-i(\omega_2 - \omega_1)t + i(\omega_2 - \omega_{n,j})\tau} |g_{n,j}|^2 (n(\omega_{n,j}, T_j) + 1) \\ & + \rho(t) V_{j,1} V_{j,1}^\dagger e^{i(\omega_1 - \omega_{n,j})\tau} |g_{n,j}|^2 n(\omega_{n,j}, T_j) + \rho(t) V_{j,1} V_{j,2}^\dagger e^{-i(\omega_1 - \omega_2)t + i(\omega_1 - \omega_{n,j})\tau} |g_{n,j}|^2 n(\omega_{n,j}, T_j) \\ & + \rho(t) V_{j,2} V_{j,2}^\dagger e^{i(\omega_2 - \omega_{n,j})\tau} |g_{n,j}|^2 n(\omega_{n,j}, T_j) + \rho(t) V_{j,2} V_{j,1}^\dagger e^{-i(\omega_2 - \omega_1)t + i(\omega_2 - \omega_{n,j})\tau} |g_{n,j}|^2 n(\omega_{n,j}, T_j) \\ & - V_{j,1}^\dagger \rho(t) V_{j,1} e^{i(\omega_1 - \omega_{n,j})\tau} |g_{n,j}|^2 n(\omega_{n,j}, T_j) - V_{j,1}^\dagger \rho(t) V_{j,2} e^{-i(\omega_2 - \omega_1)t + i(\omega_2 - \omega_{n,j})\tau} |g_{n,j}|^2 n(\omega_{n,j}, T_j) \\ & - V_{j,2}^\dagger \rho(t) V_{j,2} e^{i(\omega_2 - \omega_{n,j})\tau} |g_{n,j}|^2 n(\omega_{n,j}, T_j) - V_{j,2}^\dagger \rho(t) V_{j,1} e^{-i(\omega_1 - \omega_2)t + i(\omega_1 - \omega_{n,j})\tau} |g_{n,j}|^2 n(\omega_{n,j}, T_j)]. \end{aligned} \quad (2.16)$$

In order to evaluate the expression above, the summation over the reservoir state oscillators is changed to an integral by using the spectral density $J_j(\omega)$ such that

$$\sum_n |g_{n,j}|^2 \delta(\omega - \omega_{n,j}) \rightarrow \int_0^\infty d\omega J_j(\omega).$$

As an illustration, the first term in (2.16) can now be written as

$$\begin{aligned} & \sum_j V_{j,1} V_{j,1}^\dagger \rho(t) \int_0^\infty d\omega J_j(\omega) n(\omega_j, T_j) \int_0^\infty d\tau e^{-i(\omega - \omega_1)\tau} \\ & = \sum_j V_{j,1} V_{j,1}^\dagger \rho(t) \int_0^\infty d\omega J_j(\omega) n(\omega_j, T_j) (\pi \delta(\omega - \omega_1) + i \frac{P}{\omega_1 - \omega}). \end{aligned}$$

In the equation above, we have made use of

$$\int_0^\infty dx e^{\pm ikx} = \pi \delta(k) \pm i \frac{P}{k}, \quad (2.17)$$

where P indicates the Cauchy principal value [24].

The expression (2.16) can be simplified further by neglecting the rapidly oscillating terms containing $e^{\pm i(\omega_1 \pm \omega_2)t}$ [5]. Noting that

$$\int_0^\infty d\omega J_j(\omega) \pi \delta(\omega - \omega_i) = \pi J_j(\omega_i), \quad (2.18)$$

the equation of motion can now be written as

$$\begin{aligned} \frac{d}{dt} \tilde{\rho} = & - \sum_{i,j=1}^2 [(\pi J_j(\omega_i) n(\omega_i, T_j) + iP \int_0^\infty d\omega \frac{J_j(\omega)}{\omega - \omega_i}) n(\omega_i, T_j) V_{j,i} V_{j,i}^\dagger \rho(t) \\ & - (\pi J_j(\omega_i) n(\omega_i, T_j) + iP \int_0^\infty d\omega \frac{J_j(\omega)}{\omega - \omega_i}) n(\omega_i, T_j) V_{j,i}^\dagger \rho(t) V_{j,i} \\ & + (\pi J_j(\omega_i) (n(\omega_i, T_j) + 1) + iP \int_0^\infty d\omega \frac{J_j(\omega)}{\omega - \omega_i}) (n(\omega_i, T_j) + 1) \rho(t) V_{j,i} V_{j,i}^\dagger \\ & - (\pi J_j(\omega_i) (n(\omega_i, T_j) + 1) + iP \int_0^\infty d\omega \frac{J_j(\omega)}{\omega - \omega_i}) (n(\omega_i, T_j) + 1) V_{j,i} \rho(t) V_{j,i}^\dagger \\ & + (\pi J_j(\omega_i) (n(\omega_i, T_j) + 1) - iP \int_0^\infty d\omega \frac{J_j(\omega)}{\omega - \omega_i}) (n(\omega_i, T_j) + 1) V_{j,i}^\dagger V_{j,i} \rho(t) \\ & - (\pi J_j(\omega_i) (n(\omega_i, T_j) + 1) - iP \int_0^\infty d\omega \frac{J_j(\omega)}{\omega - \omega_i}) (n(\omega_i, T_j) + 1) V_{j,i} \rho(t) V_{j,i}^\dagger \\ & + (\pi J_j(\omega_i) n(\omega_i, T_j) - iP \int_0^\infty d\omega \frac{J_j(\omega)}{\omega - \omega_i}) (n(\omega_i, T_j) + 1) \rho(t) V_{j,i} V_{j,i}^\dagger \\ & - (\pi J_j(\omega_i) n(\omega_i, T_j) - iP \int_0^\infty d\omega \frac{J_j(\omega)}{\omega - \omega_i}) (n(\omega_i, T_j) + 1) V_{j,i}^\dagger \rho(t) V_{j,i}]. \end{aligned} \quad (2.19)$$

Introducing commutators and anti-commutators of the $V_{j,i}$ and $V_{j,i}^\dagger$, the above expression can now be compactly stated as

$$\begin{aligned} \frac{d}{dt} \tilde{\rho} = & \sum_{i,j=1}^2 [(2\pi J_j(\omega_i) n(\omega_i, T_j) (V_{j,i}^\dagger \rho(t) V_{j,i} - \frac{1}{2} \{V_{j,i} V_{j,i}^\dagger, \rho(t)\})_+ \\ & + (2\pi J_j(\omega_i) (n(\omega_i, T_j) + 1) (V_{j,i} \rho(t) V_{j,i}^\dagger - \frac{1}{2} \{V_{j,i}^\dagger V_{j,i}, \rho(t)\})_+ \\ & - iP \int_0^\infty d\omega \frac{J_j(\omega)}{\omega - \omega_i}) n(\omega_i, T_j) [V_{j,i} V_{j,i}^\dagger, \rho(t)] - iP \int_0^\infty d\omega \frac{J_j(\omega)}{\omega - \omega_i}) (n(\omega_i, T_j) + 1) [V_{j,i}^\dagger V_{j,i}, \rho(t)]. \end{aligned} \quad (2.20)$$

The last two terms on the right hand side of (2.20) constitute the Lamb shift effects that can be neglected [5]. The first two constitute the dissipator $D(\rho)$, i.e.

$$D(\rho) = \sum_{i,j=1}^2 [(2\pi J_j(\omega_i) n(\omega_i, T_j) (V_{j,i}^\dagger \rho(t) V_{j,i} - \frac{1}{2} \{V_{j,i} V_{j,i}^\dagger, \rho(t)\})_+]$$

$$+(2\pi J_j(\omega_i)(n(\omega_i, T_j) + 1)(V_{j,i}\rho(t)V_{j,i}^\dagger - \frac{1}{2}\{V_{j,i}^\dagger V_{j,i}, \rho(t)\}_+)]. \quad (2.21)$$

The above expression is written in the Schrödinger picture as [17]

$$\dot{\rho} = -i[H_S, \rho] + D(\rho). \quad (2.22)$$

Thus, the equation of motion for the two-spin system has been put in the form (1.28). A similar result would be obtained for a higher spin system. The three-spin system will be studied in Section 2.4.

For easy analysis of the two-spin system, a basis in which the system Hamiltonian H_S is diagonal is convenient. The basis used is $|0\rangle$ and $|1\rangle$ such that:

$$|0\rangle = \begin{pmatrix} 0 \\ 1 \end{pmatrix}; \quad |1\rangle = \begin{pmatrix} 1 \\ 0 \end{pmatrix}$$

and, as an example,

$$|01\rangle = \begin{pmatrix} 0 \\ 1 \end{pmatrix} \otimes \begin{pmatrix} 1 \\ 0 \end{pmatrix}.$$

The four eigenvalues of the Hamiltonian given by Eq.(2.3) and their respective eigenvectors thus become:

$$\begin{aligned} \lambda_1 &= -\frac{1}{2}(\epsilon_1 + \epsilon_2); & |\lambda_1\rangle &= |00\rangle, \\ \lambda_2 &= \frac{1}{2}(\epsilon_1 + \epsilon_2); & |\lambda_2\rangle &= |11\rangle, \\ \lambda_3 &= -\frac{1}{2}\sqrt{(\epsilon_1 - \epsilon_2)^2 + 4K^2}; & |\lambda_3\rangle &= \cos\theta|10\rangle + \sin\theta|01\rangle, \\ \lambda_4 &= \frac{1}{2}\sqrt{(\epsilon_1 - \epsilon_2)^2 + 4K^2}; & |\lambda_4\rangle &= -\sin\theta|10\rangle + \cos\theta|01\rangle, \end{aligned}$$

where

$$\tan 2\theta = \frac{2K}{\epsilon_1 - \epsilon_2}.$$

This gives, using (2.6) and (2.7), the result that in the $|\lambda_i\rangle$ basis, the transition operators, $V_{j,i}^\dagger$ and $V_{j,i}$ are

$$\begin{aligned}
\hat{V}_{1,1}^\dagger &= \sin \theta [|\lambda_2\rangle\langle\lambda_3| - |\lambda_4\rangle\langle\lambda_1|] \\
\hat{V}_{1,2}^\dagger &= \cos \theta [|\lambda_3\rangle\langle\lambda_1| + |\lambda_2\rangle\langle\lambda_4|] \\
\hat{V}_{2,1}^\dagger &= \cos \theta [|\lambda_2\rangle\langle\lambda_3| + |\lambda_4\rangle\langle\lambda_1|] \\
\hat{V}_{2,2}^\dagger &= \sin \theta [|\lambda_3\rangle\langle\lambda_1| - |\lambda_2\rangle\langle\lambda_4|] \\
\hat{V}_{1,1} &= \sin \theta [|\lambda_3\rangle\langle\lambda_2| - |\lambda_1\rangle\langle\lambda_4|] \\
\hat{V}_{1,2} &= \cos \theta [|\lambda_1\rangle\langle\lambda_3| + |\lambda_4\rangle\langle\lambda_2|] \\
\hat{V}_{2,1} &= \cos \theta [|\lambda_3\rangle\langle\lambda_2| + |\lambda_1\rangle\langle\lambda_4|] \\
\hat{V}_{2,2} &= \sin \theta [|\lambda_1\rangle\langle\lambda_3| - |\lambda_4\rangle\langle\lambda_2|].
\end{aligned} \tag{2.23}$$

The transition frequencies are:

$$\omega_1 = (\epsilon + \Delta)$$

and

$$\omega_2 = (\epsilon - \Delta),$$

where

$$\epsilon = \frac{1}{2}(\epsilon_1 + \epsilon_2)$$

and

$$\Delta = \frac{1}{2}\sqrt{(\epsilon_1 - \epsilon_2)^2 + 4K^2}.$$

It should be noted that the above is true for the case where $\epsilon > \Delta$. With the transition operators (2.23), Eq.(2.22) can now be used to explicitly find the equation of motion of the reduced density matrix. Several elements of the matrix are seen to be linearly linked. For each set of such linked elements, an equation can be written of the form:

$$\frac{d}{dt} \hat{\rho}(t) = A \hat{\rho}(t) , \tag{2.24}$$

where A is a square matrix with constant coefficients.

It follows, therefore, that

$$\rho(t) = e^{At} \rho(0). \tag{2.25}$$

Thus the solution can be found for all the elements of the density matrix. The solution for the diagonal elements is given by:

$$\frac{d}{dt} \hat{\rho}(t) = M \hat{\rho}(t) , \quad (2.26)$$

where M is the coefficient matrix:

$$\begin{pmatrix} -(A^+ + B^+) & 0 & A^- & B^- \\ 0 & -(-B^- + A^-) & B^+ & A^+ \\ A^+ & B^- & -(B^+ + A^-) & 0 \\ B^+ & A^- & 0 & -(A^+ + B^-) \end{pmatrix} .$$

This equation is solved using (2.25) to give

$$\rho_{ii}(t) = \frac{1}{AB} \begin{pmatrix} a_{11} & a_{12} & a_{13} & a_{14} \\ a_{21} & a_{22} & a_{23} & a_{24} \\ a_{31} & a_{32} & a_{33} & a_{34} \\ a_{41} & a_{42} & a_{43} & a_{44} \end{pmatrix} \begin{pmatrix} \rho_{11}(0) \\ \rho_{22}(0) \\ \rho_{33}(0) \\ \rho_{44}(0) \end{pmatrix} ,$$

where the components of the above matrix are:

$$\begin{aligned} a_{11} &= (B^+ e^{-Bt} + B^-)(A^+ e^{-At} + A^-), \\ a_{12} &= (-e^{-Bt} + 1)(-e^{-At} + 1)B^- A^-, \\ a_{13} &= A^-(B^+ e^{-Bt} + B^-)(-e^{-At} + 1), \\ a_{14} &= B^-(-e^{-Bt} + 1)(A^+ e^{-At} + A^-), \\ a_{21} &= A^+ B^+(-e^{-Bt} + 1)(-e^{-At} + 1), \\ a_{22} &= (B^- e^{-Bt} + B^+)(A^- e^{-At} + A^+), \\ a_{23} &= B^+(-e^{-Bt} + 1)(A^- e^{-At} + A^+), \\ a_{24} &= A^+(B^- e^{-Bt} + B^+)(-e^{-At} + 1), \\ a_{31} &= A^+(B^+ e^{-Bt} + B^-)(-e^{-At} + 1), \\ a_{32} &= B^-(-e^{-Bt} + 1)(A^- e^{-At} + A^+), \end{aligned}$$

$$\begin{aligned}
a_{33} &= (B^+ e^{-Bt} + B^-)(A^- e^{-At} + A^+), \\
a_{34} &= A^+ B^- (-e^{-Bt} + 1)(-e^{-At} + 1), \\
a_{41} &= B^+ (-e^{-Bt} + 1)(A^+ e^{-At} + A^-), \\
a_{42} &= A^- (B^- e^{-Bt} + B^+)(-e^{-At} + 1), \\
a_{43} &= B^+ A^- (-e^{-Bt} + 1)(-e^{-At} + 1), \\
a_{44} &= (B^- e^{-Bt} + B^+)(A^+ e^{-At} + A^-).
\end{aligned}$$

In the above expressions, we have introduced

$$\begin{aligned}
A^+ &= 2\pi J_1(\omega_2) n(T_1, \omega_2) \cos^2 \theta + 2\pi J_2(\omega_2) n(T_2, \omega_2) \sin^2 \theta, \\
B^+ &= 2\pi J_2(\omega_1) n(T_2, \omega_1) \cos^2 \theta + 2\pi J_1(\omega_1) n(T_1, \omega_1) \sin^2 \theta, \\
B^- &= 2\pi J_2(\omega_1) (n(T_2, \omega_1) + 1) \cos^2 \theta + 2\pi J_1(\omega_1) (n(T_1, \omega_1) + 1) \sin^2 \theta, \\
A^- &= 2\pi J_1(\omega_2) (n(T_1, \omega_2) + 1) \cos^2 \theta + 2\pi J_2(\omega_2) (n(T_2, \omega_2) + 1) \sin^2 \theta,
\end{aligned}$$

$$A = A^+ + A^-,$$

and

$$B = B^+ + B^-.$$

T_j and J_j are the temperature and spectral density values for the respective baths. From the above matrix elements, it is observed that as time increases to very large values simple expressions are found for the asymptotic values of the components:

$$\begin{aligned}
\lim_{t \rightarrow \infty} a_{11} &= \lim_{t \rightarrow \infty} a_{12} = \lim_{t \rightarrow \infty} a_{13} = \lim_{t \rightarrow \infty} a_{14} = \frac{A^- B^-}{AB}, \\
\lim_{t \rightarrow \infty} a_{21} &= \lim_{t \rightarrow \infty} a_{22} = \lim_{t \rightarrow \infty} a_{23} = \lim_{t \rightarrow \infty} a_{24} = \frac{A^+ B^+}{AB}, \\
\lim_{t \rightarrow \infty} a_{31} &= \lim_{t \rightarrow \infty} a_{32} = \lim_{t \rightarrow \infty} a_{33} = \lim_{t \rightarrow \infty} a_{34} = \frac{A^+ B^-}{AB}, \\
\lim_{t \rightarrow \infty} a_{41} &= \lim_{t \rightarrow \infty} a_{42} = \lim_{t \rightarrow \infty} a_{43} = \lim_{t \rightarrow \infty} a_{44} = \frac{A^- B^+}{AB}.
\end{aligned}$$

Given the fact that the trace of the density matrix is unity, the expressions above lead to the result

$$\lim_{t \rightarrow \infty} (\rho_{ii}) = \frac{1}{AB} \begin{pmatrix} A^- B^- \\ A^+ B^+ \\ A^+ B^- \\ A^- B^+ \end{pmatrix}.$$

As will be shown rigorously in the next section, the non-diagonal elements of the density matrix vanish to zero as time increases to very large values. This shows that the solution of the density matrix for large values of time is a diagonal density matrix.

2.4 The Three-Spin System

The treatment for a three-spin system is similar to that of a two-spin system. For this particular case, it is assumed that all the energy levels have the same magnitude ϵ_o . Like in the two-spin system, it is also assumed that two of the three spins are coupled to two bosonic baths at temperatures T_1 and T_2 . This allows for simplification of the study as only transition operators and frequencies for those two spins will be required for a complete analysis. It is also assumed that the spin-spin interaction strength K is the same between all spins. This leads, using (2.3) to the Hamiltonian below

$$\hat{H}_s = \sum_i^3 \frac{\epsilon_o}{2} \sigma_i^z + K \sum_i^2 (\sigma_i^+ \sigma_{i+1}^- + \sigma_i^- \sigma_{i+1}^+). \quad (2.27)$$

As for the two-spin system, the analysis is best done in the basis that diagonalizes the Hamiltonian. In the basis that was used for the two-spin system, the eigenvalues of the Hamiltonian

and their respective eigenvectors are:

$$\begin{aligned}
\lambda_1 &= -\frac{3}{2}\epsilon_o; & |\lambda_1\rangle &= |000\rangle, \\
\lambda_2 &= -\frac{\epsilon_o}{2}; & |\lambda_2\rangle &= \frac{1}{\sqrt{2}}(|001\rangle - |100\rangle), \\
\lambda_3 &= \frac{\epsilon_o}{2}; & |\lambda_3\rangle &= \frac{1}{\sqrt{2}}(|011\rangle - |110\rangle), \\
\lambda_4 &= \frac{3}{2}\epsilon_o; & |\lambda_4\rangle &= |111\rangle, \\
\lambda_5 &= -\frac{1}{2}(\epsilon_o + 2\sqrt{2}K); & |\lambda_5\rangle &= \frac{1}{\sqrt{2}}(|100\rangle - \frac{2}{\sqrt{2}}|010\rangle + |001\rangle), \\
\lambda_6 &= \frac{1}{2}(\epsilon_o - 2\sqrt{2}K); & |\lambda_6\rangle &= \frac{1}{\sqrt{2}}(|110\rangle - \frac{2}{\sqrt{2}}|101\rangle + |011\rangle), \\
\lambda_7 &= -\frac{1}{2}(\epsilon_o - 2\sqrt{2}K); & |\lambda_7\rangle &= \frac{1}{\sqrt{2}}(|100\rangle + \frac{2}{\sqrt{2}}|010\rangle + |001\rangle), \\
\lambda_8 &= \frac{1}{2}(\epsilon_o + 2\sqrt{2}K); & |\lambda_8\rangle &= \frac{1}{\sqrt{2}}(|110\rangle + \frac{2}{\sqrt{2}}|101\rangle + |011\rangle).
\end{aligned}$$

Here (2.7) and (2.8) are used to determine the transition operators for this system. It is found that

$$\begin{aligned}
\hat{V}_{11}^\dagger &= \frac{1}{\sqrt{2}}[|\lambda_4\rangle\langle\lambda_3| - |\lambda_2\rangle\langle\lambda_1| - |\lambda_6\rangle\langle\lambda_5| + |\lambda_8\rangle\langle\lambda_7|], \\
\hat{V}_{12}^\dagger &= \frac{1}{2}[|\lambda_3\rangle\langle\lambda_5| + |\lambda_4\rangle\langle\lambda_6| + |\lambda_7\rangle\langle\lambda_1| + |\lambda_8\rangle\langle\lambda_2|], \\
\hat{V}_{13}^\dagger &= \frac{1}{2}[|\lambda_4\rangle\langle\lambda_8| - |\lambda_3\rangle\langle\lambda_7| + |\lambda_5\rangle\langle\lambda_1| - |\lambda_6\rangle\langle\lambda_2|], \\
\hat{V}_{31}^\dagger &= \frac{1}{\sqrt{2}}[|\lambda_2\rangle\langle\lambda_1| - |\lambda_4\rangle\langle\lambda_3| - |\lambda_6\rangle\langle\lambda_5| + |\lambda_8\rangle\langle\lambda_7|], \\
\hat{V}_{32}^\dagger &= \frac{1}{2}[|\lambda_4\rangle\langle\lambda_6| - |\lambda_3\rangle\langle\lambda_5| - |\lambda_8\rangle\langle\lambda_2| + |\lambda_7\rangle\langle\lambda_1|], \\
\hat{V}_{33}^\dagger &= \frac{1}{2}[|\lambda_3\rangle\langle\lambda_7| + |\lambda_4\rangle\langle\lambda_8| + |\lambda_5\rangle\langle\lambda_1| + |\lambda_6\rangle\langle\lambda_2|],
\end{aligned}$$

$$\begin{aligned}
\hat{V}_{11} &= \frac{1}{\sqrt{2}}[|\lambda_3\rangle\langle\lambda_4| - |\lambda_1\rangle\langle\lambda_2| - |\lambda_5\rangle\langle\lambda_6| + |\lambda_7\rangle\langle\lambda_8|], \\
\hat{V}_{12} &= \frac{1}{2}[|\lambda_5\rangle\langle\lambda_3| + |\lambda_6\rangle\langle\lambda_4| + |\lambda_1\rangle\langle\lambda_7| + |\lambda_2\rangle\langle\lambda_8|], \\
\hat{V}_{13} &= \frac{1}{2}[|\lambda_8\rangle\langle\lambda_4| - |\lambda_7\rangle\langle\lambda_3| + |\lambda_1\rangle\langle\lambda_5| - |\lambda_2\rangle\langle\lambda_6|], \\
\hat{V}_{31} &= \frac{1}{\sqrt{2}}[|\lambda_1\rangle\langle\lambda_2| - |\lambda_3\rangle\langle\lambda_4| - |\lambda_5\rangle\langle\lambda_6| + |\lambda_7\rangle\langle\lambda_8|], \\
\hat{V}_{32} &= \frac{1}{2}[|\lambda_6\rangle\langle\lambda_4| - |\lambda_5\rangle\langle\lambda_3| - |\lambda_2\rangle\langle\lambda_8| + |\lambda_1\rangle\langle\lambda_7|], \\
\hat{V}_{33} &= \frac{1}{2}[|\lambda_7\rangle\langle\lambda_3| + |\lambda_8\rangle\langle\lambda_4| + |\lambda_1\rangle\langle\lambda_5| + |\lambda_2\rangle\langle\lambda_6|].
\end{aligned}$$

The transition frequencies are

$$\begin{aligned}
\omega_1 &= \epsilon_o, \\
\omega_2 &= \epsilon_o + \sqrt{2}K, \\
\omega_3 &= \epsilon_o - \sqrt{2}K.
\end{aligned}$$

As in the previous case, (2.25) is used for an analytical treatment of the diagonal elements to give

$$\rho_{ii}(t) = \frac{1}{XYZ} \begin{pmatrix} \alpha_{11} & \alpha_{12} & \cdots & \alpha_{18} \\ \alpha_{21} & \ddots & \cdots & \vdots \\ \vdots & \cdots & \ddots & \vdots \\ \alpha_{81} & \cdots & \cdots & \alpha_{88} \end{pmatrix} \begin{pmatrix} \rho_{11}(0) \\ \rho_{22}(0) \\ \vdots \\ \rho_{88}(0) \end{pmatrix},$$

where the matrix components are explicitly:

$$\begin{aligned}
\alpha_{11} &= (X^+ - e^{-Xt}X^-)(Y^+ - e^{-Yt}Y^-)(Z^+ - e^{-Zt}Z^-), \\
\alpha_{12} &= (1 - e^{-Xt})X^+(Y^+ - e^{-Yt}Y^-)(Z^+ - e^{-Zt}Z^-), \\
\alpha_{13} &= (1 - e^{-Yt})(1 - e^{-Zt})Y^+Z^+(X^+ - e^{-Xt}X^-), \\
\alpha_{14} &= (1 - e^{-Xt})(1 - e^{-Yt})(1 - e^{-Zt})X^+Y^+Z^+, \\
\alpha_{15} &= (1 - e^{-Zt})Z^+(X^+ - e^{-Xt}X^-)(Y^+ - e^{-Yt}Y^-), \\
\alpha_{16} &= (1 - e^{-Xt})(1 - e^{-Zt})X^+Z^+(Y^+ - e^{-Yt}Y^-), \\
\alpha_{17} &= (1 - e^{-Yt})Y^+(X^+ - e^{-Xt}X^-)(Z^+ - e^{-Zt}Z^-), \\
\alpha_{18} &= (1 - e^{-Xt})(1 - e^{-Yt})X^+Y^+(Z^+ - e^{-Zt}Z^+),
\end{aligned}$$

$$\begin{aligned}
\alpha_{21} &= (1 - e^{-Xt})X^-(Y^+ - e^{-Yt}Y^-)(Z^+ - e^{-Zt}Z^-), \\
\alpha_{22} &= (X^- - e^{-Xt}X^+)(Y^+ - e^{-Yt}Y^-)(Z^+ - e^{-Zt}Z^-), \\
\alpha_{23} &= (1 - e^{-Xt})(1 - e^{-Yt})(1 - e^{-Zt})Y^+Z^+X^-, \\
\alpha_{24} &= (1 - e^{-Yt})(1 - e^{-Zt})Y^+Z^+(X^- - e^{-Xt}X^+), \\
\alpha_{25} &= (1 - e^{-Xt})(1 - e^{-Zt})X^-Z^+(Y^+ - e^{-Yt}Y^-), \\
\alpha_{26} &= (1 - e^{-Zt})Z^+(X^- - e^{-Xt}X^+)(Y^+ - e^{-Yt}Y^-), \\
\alpha_{27} &= (1 - e^{-Xt})(1 - e^{-Yt})Y^+X^-(Z^+ - e^{-Zt}Z^-), \\
\alpha_{28} &= (1 - e^{-Yt})Y^+(X^- - e^{-Xt}X^+)Y^+(Z^+ - e^{-Zt}Z^-), \\
\alpha_{31} &= (1 - e^{-Yt})(1 - e^{-Zt})(X^+ - e^{-Xt}X^-)Y^-Z^-, \\
\alpha_{32} &= (1 - e^{-Xt})(1 - e^{-Yt})(1 - e^{-Zt})X^+Y^-Z^-, \\
\alpha_{33} &= (X^+ - e^{-Xt}X^-)(Y^- - e^{-Yt}Y^+)(Z^- - e^{-Zt}Z^+), \\
\alpha_{34} &= (1 - e^{-Xt})X^+(Y^- - e^{-Yt}Y^+)(Z^- - e^{-Zt}Z^+), \\
\alpha_{35} &= (1 - e^{-Yt})(X^+ - e^{-Xt}X^-)Y^-(Z^- - e^{-Zt}Z^+), \\
\alpha_{36} &= (1 - e^{-Xt})(1 - e^{-Yt})X^+Y^-(Z^- - e^{-Zt}Z^+), \\
\alpha_{37} &= (1 - e^{-Zt})(X^+ - e^{-Xt}X^-)(Y^- - e^{-Yt}Y^+)Z^-, \\
\alpha_{38} &= (1 - e^{-Xt})(1 - e^{-Zt})X^+(Y^- - e^{-Yt}Y^+)Z^-, \\
\alpha_{41} &= (1 - e^{-Xt})(1 - e^{-Yt})(1 - e^{-Zt})X^-Y^-Z^-, \\
\alpha_{42} &= (1 - e^{-Yt})(1 - e^{-Zt})(X^- - e^{-Xt}X^+)Y^-Z^-, \\
\alpha_{43} &= (1 - e^{-Xt})X^-(Y^- - e^{-Yt}Y^+)(Z^- - e^{-Zt}Z^+), \\
\alpha_{44} &= (X^- - e^{-Xt}X^+)(Y^- - e^{-Yt}Y^+)(Y^- - e^{-Zt}Z^+), \\
\alpha_{45} &= (1 - e^{-Xt})(1 - e^{-Yt})X^-Y^-(Z^- - e^{-Zt}Z^+), \\
\alpha_{46} &= (1 - e^{-Yt})(X^- - e^{-Xt}X^+)Y^-(Z^- - e^{-Zt}Z^+), \\
\alpha_{47} &= (1 - e^{-Xt})(1 - e^{-Zt})X^-(Y^- - e^{-Yt}Y^+)Z^-, \\
\alpha_{48} &= (1 - e^{-Zt})(X^- - e^{-Xt}X^+)(Y^- - e^{-Yt}Y^+)Z^-, \\
\alpha_{51} &= (1 - e^{-Zt})(X^+ - e^{-Xt}X^-)(Y^+ - e^{-Yt}Y^-)Z^-, \\
\alpha_{52} &= (1 - e^{-Xt})(1 - e^{-Zt})X^+(Y^+ - e^{-Yt}Y^-)Z^-,
\end{aligned}$$

$$\begin{aligned}
\alpha_{53} &= (1 - e^{-Yt})(X^+ - e^{-Xt}X^+)Y^+(Z^- - e^{-Zt}Z^+), \\
\alpha_{54} &= (1 - e^{-Xt})(1 - e^{-Yt})X^+Y^+(Z^- - e^{-Zt}Z^+), \\
\alpha_{55} &= (X^+ - e^{-Xt}X^+)(Y^+ - e^{-Yt}Y^+)(Z^- - e^{-Zt}Z^+), \\
\alpha_{56} &= (1 - e^{-Xt})X^+(Y^+ - e^{-Yt}Y^-)(Z^- - e^{-Zt}Z^+), \\
\alpha_{57} &= (1 - e^{-Yt})(1 - e^{-Zt})Y^+(X^+ - e^{-Xt}X^-)Z^-, \\
\alpha_{58} &= (1 - e^{-Xt})(1 - e^{-Yt})(1 - e^{-Zt})X^+Y^+Z^-, \\
\alpha_{61} &= (1 - e^{-Xt})(1 - e^{-Zt})X^-(Y^+ - e^{-Yt}Y^-)Z^-, \\
\alpha_{62} &= (1 - e^{-Zt})(X^- - e^{-Xt}X^+)(Y^+ - e^{-Yt}Y^-)Z^-, \\
\alpha_{63} &= (1 - e^{-Xt})(1 - e^{-Yt})Y^+X^-(Z^- - e^{-Zt}Z^+), \\
\alpha_{64} &= (1 - e^{-Yt})Y^+(X^- - e^{-Xt}X^+)(Z^- - e^{-Zt}Z^+), \\
\alpha_{65} &= (1 - e^{-Xt})X^-(Y^+ - e^{-Yt}Y^-)(Z^- - e^{-Zt}Z^+), \\
\alpha_{66} &= (X^- - e^{-Xt}X^+)(Y^+ - e^{-Yt}Y^-)(Z^- - e^{-Zt}Z^+), \\
\alpha_{67} &= (1 - e^{-Xt})(1 - e^{-Yt})(1 - e^{-Zt})Y^+X^-Z^-, \\
\alpha_{68} &= (1 - e^{-Yt})(1 - e^{-Zt})Y^+(X^- - e^{-Xt}X^+)Z^-, \\
\alpha_{71} &= (1 - e^{-Yt})(X^+ - e^{-Xt}X^-)Y^-(Z^+ - e^{-Zt}Z^-), \\
\alpha_{72} &= (1 - e^{-Xt})(1 - e^{-Yt})X^+Y^-(Z^+ - e^{-Zt}Z^-), \\
\alpha_{73} &= (1 - e^{-Zt})Z^+(X^+ - e^{-Xt}X^-)(Y^- - e^{-Yt}Y^+), \\
\alpha_{74} &= (1 - e^{-Xt})(1 - e^{-Zt})X^+Z^+(Y^- - e^{-Yt}Y^+), \\
\alpha_{75} &= (1 - e^{-Yt})(1 - e^{-Zt})Z^+(X^+ - e^{-Xt}X^-)Y^-, \\
\alpha_{76} &= (1 - e^{-Xt})(1 - e^{-Yt})(1 - e^{-Zt})X^+Z^+Y^-, \\
\alpha_{77} &= (X^+ - e^{-Xt}X^-)(Y^- - e^{-Yt}Y^+)(Z^+ - e^{-Zt}Z^-), \\
\alpha_{78} &= (1 - e^{-Xt})X^+(Y^- - e^{-Yt}Y^+)(Z^+ - e^{-Zt}Z^-), \\
\alpha_{81} &= (1 - e^{-Xt})(1 - e^{-Yt})X^-Y^-(Z^+ - e^{-Zt}Z^-), \\
\alpha_{82} &= (1 - e^{-Yt})(X^- - e^{-Xt}X^+)Y^-(Z^+ - e^{-Zt}Z^-), \\
\alpha_{83} &= (1 - e^{-Xt})Z^+X^-(1 - e^{-Zt})(Y^- - e^{-Yt}Y^+), \\
\alpha_{84} &= (X^- - e^{-Xt}X^+)Z^+(Y^- - e^{-Yt}Y^+)(1 - e^{-Yt}),
\end{aligned}$$

$$\begin{aligned}
\alpha_{85} &= (1 - e^{-Xt})(1 - e^{-Yt})(1 - e^{-Zt})Z^+X^-Y^-, \\
\alpha_{86} &= (X^- - e^{-Xt}X^+)Y^-(1 - e^{-Yt})Z^+(1 - e^{-Zt}), \\
\alpha_{87} &= (1 - e^{-Xt})X^-(Y^- - e^{-Yt}Y^+)(Z^+ - e^{-Zt}Z^-), \\
\alpha_{88} &= (X^- - e^{-Xt}X^+)(Y^- - e^{-Yt}Y^+)(Z^+ - e^{-Zt}Z^-).
\end{aligned}$$

In the above expressions we have used the abbreviations:

$$\begin{aligned}
X^\mp &= \pi J_1(\pm\omega_1)n(T_1, \pm\omega_1) + \pi J_2(\pm\omega_1)n(T_2, \pm\omega_1), \\
Y^\mp &= \frac{\pi}{2}J_1(\pm\omega_2)n(T_1, \pm\omega_2) + \frac{\pi}{2}J_2(\pm\omega_2)n(T_2, \pm\omega_2), \\
Z^\mp &= \frac{\pi}{2}J_1(\pm\omega_3)n(T_1, \pm\omega_3) + \frac{\pi}{2}J_2(\pm\omega_3)n(T_2, \pm\omega_3), \\
X^+ + X^- &= X, \\
Y^+ + Y^- &= Y
\end{aligned}$$

and

$$Z^+ + Z^- = Z.$$

As in the two-spin case, T_i and J_i are the temperature and spectral density respectively for the j^{th} bath. An analysis is now done to see what happens to the elements of the density matrix when time becomes large. It is easy to see that:

$$\begin{aligned}
\lim_{t \rightarrow \infty} \alpha_{1i} &= \frac{X^+Y^+Z^+}{XYZ}, \\
\lim_{t \rightarrow \infty} \alpha_{2i} &= \frac{X^-Y^+Z^+}{XYZ}, \\
\lim_{t \rightarrow \infty} \alpha_{3i} &= \frac{X^+Y^-Z^-}{XYZ}, \\
\lim_{t \rightarrow \infty} \alpha_{4i} &= \frac{X^-Y^-Z^-}{XYZ}, \\
\lim_{t \rightarrow \infty} \alpha_{5i} &= \frac{X^+Y^+Z^-}{XYZ}, \\
\lim_{t \rightarrow \infty} \alpha_{6i} &= \frac{X^-Y^+Z^-}{XYZ}, \\
\lim_{t \rightarrow \infty} \alpha_{7i} &= \frac{X^+Y^-Z^+}{XYZ},
\end{aligned}$$

$$\lim_{t \rightarrow \infty} \alpha_{8i} = \frac{X^- Y^- Z^+}{XYZ}.$$

In the above expressions the index i runs from 1 to 8. Like for the 2-spin case, the above expressions imply that we have

$$\lim_{t \rightarrow \infty} (\rho_{ii}) = \frac{1}{XYZ} \begin{pmatrix} X^+ Y^+ Z^+ \\ X^- Y^+ Z^+ \\ X^+ Y^- Z^- \\ X^- Y^- Z^- \\ X^+ Y^+ Z^- \\ X^- Y^+ Z^- \\ X^+ Y^- Z^+ \\ X^- Y^- Z^+ \end{pmatrix}.$$

The evolution of the non-diagonal elements of $\rho(t)$ is now looked at. An analysis of ρ_{25} and ρ_{83} gives a demonstration of how this can be done. It is seen that ρ_{25} and ρ_{83} are linked in such a way that

$$\frac{d}{dt} \begin{pmatrix} \rho_{25}(t) \\ \rho_{83}(t) \end{pmatrix} = A_1 \begin{pmatrix} \rho_{25}(t) \\ \rho_{83}(t) \end{pmatrix},$$

where

$$A = (\Delta_1 I + M_1),$$

$$\Delta_1 = -\frac{1}{2}(X^+ + Z^+ + X^- + Y^- + Z^-) - i\sqrt{2}K,$$

I is the identity matrix, and

$$M_1 = \begin{pmatrix} -Y^- & Y^+ \\ Y^- & -Y^+ \end{pmatrix}.$$

The eigenvalues λ_i of M_1 are 0 and $-(Y^+ + Y^-)$.

The fact that $\text{Re}(\Delta_1) < 0$ and the largest eigenvalue $\lambda_{\max}(M_1) \leq 0$ means that for $i = 1, 2$

$$\text{Re}(\lambda_i(\Delta_1 I + M_1)) < 0$$

and

$$\lim_{t \rightarrow \infty} e^{tA_1} = 0.$$

Therefore, we have

$$\lim_{t \rightarrow \infty} \begin{pmatrix} \rho_{25}(t) \\ \rho_{83}(t) \end{pmatrix} = 0.$$

A similar treatment can be given to all the other sets of linked elements. For ρ_{12} , ρ_{34} , ρ_{56} and ρ_{78} ,

$$\Delta_2 = -\frac{1}{2}(X^+ + X^-) - i\epsilon_o$$

and

$$M_2 = \begin{pmatrix} -(Y^- + Z^-) & 0 & -G^+ & F^+ \\ 0 & -(Y^+ + Z^+) & F^- & -G^- \\ -G^- & F^+ & -(Z^+ + Y^-) & 0 \\ F^- & -G^+ & 0 & -(Y^+ + Z^-) \end{pmatrix}.$$

Here F^\mp , G^\mp and H^\mp are given by

$$F^\mp = \frac{\pi}{2} J_1(\pm\omega_1) n(T_1, \pm\omega_1) - \frac{\pi}{2} J_2(\pm\omega_1) n(T_2, \pm\omega_1),$$

$$G^\mp = \frac{\pi}{2} J_1(\pm\omega_2) n(T_1, \pm\omega_2) - \frac{\pi}{2} J_2(\pm\omega_2) n(T_2, \pm\omega_2),$$

$$H^\mp = \frac{\pi}{2} J_1(\pm\omega_3) n(T_1, \pm\omega_3) - \frac{\pi}{2} J_2(\pm\omega_3) n(T_2, \pm\omega_3).$$

The eigenvalues of M_2 are

$$\begin{aligned} \lambda_i &= -\frac{1}{2}(Y + Z) \pm \sqrt{Y_G^2 + Z_H^2 \pm 2Y_G Z_H}, \\ &= -\frac{1}{2}(Y + Z \pm \sqrt{(Y_G \pm Z_H)^2}), \end{aligned}$$

where

$$Y_G = \sqrt{(Y^+ - Y^-)^2 + 4G^+ G^-}$$

and

$$Z_H = \sqrt{(Z^+ - Z^-)^2 + 4H^+ H^-}.$$

Therefore, the eigenvalues

$$\lambda_i = -\frac{1}{2}(Y + Z \pm |Y_G \pm Z_H|)$$

and

$$\begin{aligned}\lambda_{\max} &= -\frac{1}{2}(Y + Z - |Y_G + Z_H|) \\ &= -\frac{1}{2}(Y - Y_G) - \frac{1}{2}(Z - Z_H).\end{aligned}$$

In order to show that

$$\lambda_{\max} \leq 0, \tag{2.28}$$

two conditions must be proved to hold. The first is that $Y - Y_G \geq 0$. This means that

$$\begin{aligned}Y^+ + Y^- &\geq \sqrt{(Y^+ - Y^-)^2 + 4G^+G^-}, \\ (Y^+ + Y^-)^2 &\geq (Y^+ - Y^-)^2 + 4G^+G^-, \\ Y^+Y^- &\geq G^+G^-, \\ Y^+Y^- - G^+G^- &\geq 0.\end{aligned}$$

But it is seen that

$$\begin{aligned}Y^+Y^- - G^+G^- &= \left(\frac{\pi}{2}J_1(-\omega_2)n(T_1, -\omega_2) + \frac{\pi}{2}J_2(-\omega_2)n(T_2, -\omega_2)\right)\left(\frac{\pi}{2}J_1(\omega_2)n(T_1, \omega_2) + \frac{\pi}{2}J_2(\omega_2)n(T_2, \omega_2)\right) \\ &\quad - \left(\frac{\pi}{2}J_1(-\omega_2)n(T_1, -\omega_2) - \frac{\pi}{2}J_2(-\omega_2)n(T_2, -\omega_2)\right)\left(\frac{\pi}{2}J_1(\omega_2)n(T_1, \omega_2) - \frac{\pi}{2}J_2(\omega_2)n(T_2, \omega_2)\right) \\ &= \pi J_1(-\omega_2)J_1(\omega_2) + \pi J_2(-\omega_2)J_1(\omega_2) \geq 0.\end{aligned}$$

This is the required result. The second condition that must be shown is that $Z - Z_H \geq 0$.

Proceeding as above, the result is obtained that

$$Z - Z_H = \pi J_1(-\omega_3)J_1(\omega_3) + \pi J_2(-\omega_3)J_1(\omega_3) \geq 0.$$

Thus it can be shown that $\lambda_{\max}(M_2) \leq 0$. Given the fact that $\text{Re}(\Delta_2) < 0$, it follows that $\text{Re}(\lambda_i(\Delta_2 I + M_2)) < 0$ for $i = 1, 2, 3, 4$.

Therefore, we can summarize the above derivations in the following compact form:

$$\lim_{t \rightarrow \infty} e^{t(\Delta_2 I + M_2)} = 0$$

and

$$\lim_{t \rightarrow \infty} \begin{pmatrix} \rho_{15}(t) \\ \rho_{34}(t) \\ \rho_{56}(t) \\ \rho_{78}(t) \end{pmatrix} = 0.$$

A similar analysis as above is repeated for all the other non-diagonal elements. The corresponding quantities Δ_i , M_i and their eigenvalues are given in the Appendix for each set of proportional matrix elements. As in the cases dealt with above, it can be shown that for $i \neq j$

$$\lim_{t \rightarrow \infty} \rho_{ij}(t) = 0. \tag{2.29}$$

This means that the non-diagonal elements vanish when time becomes large. And therefore, as in the case of the two-spin system, the solution converges to a diagonal density matrix as $t \rightarrow \infty$.

In this chapter, the strong spin-spin interaction model has been studied. In the first case, a two-spin system is interacting in such a way that each of the spins is coupled to a separate bosonic bath at a different temperature. In the three-spin case, two of the three spins are each coupled to a separate bosonic bath at a different temperature.

These two cases are simple enough to be studied analytically. Compared to a numerical approach, an analytical study of the model allows for a deeper understanding of the physical processes involved in the interaction of the qubit systems with the bosonic baths. The solutions are general and, therefore, results can be obtained for any set of parameters.

Chapter 3

The Weak Spin-Spin Interaction Model

The difference between this model and the strong spin-spin interaction model is that in this particular case, the interaction between the spins is far much weaker. A direct result of this is that the energy spectrum has a different form. Unlike in the strong interaction case, the energy levels for the spins are not brought into one composite system. The separation between them is maintained. In this case, as in the strong interaction case, the environment consists of two bosonic baths. Each spin of the sub-system is coupled to a separate bath. The interaction between each bath and the subsystem S is again given by the Hamiltonian (2.2).

Employing the Master Equation (1.39), the evolution with time of the system is given by

$$\begin{aligned} \frac{d}{dt} \tilde{\rho} = & - \sum_{n,j} \sum_{m,k} \int_0^\infty dt' [(g_{n,j} \hat{b}_{n,j}^\dagger e^{i\omega_{n,j}t} \sigma_j^- e^{-i\omega_j t} + g_{n,j}^* \hat{b}_{n,j} e^{-i\omega_{n,j}t} \sigma_j^+ e^{i\omega_j t}), \\ & [(g_{m,k} \hat{b}_{m,k}^\dagger e^{i\omega_{m,k}t'} \sigma_k^- e^{-i\omega_k t'} + g_{m,k}^* \hat{b}_{m,k} e^{-i\omega_{m,k}t'} \sigma_k^+ e^{i\omega_k t'}), \rho(t) \otimes \rho_R]]. \end{aligned} \quad (3.1)$$

The indices m , k , n and j have the same meaning as in the strong interaction case. The trace is again taken over the Hilbert space of the reservoir, and τ is introduced such that $t' = t - \tau$.

The equation of motion now becomes

$$\begin{aligned}
\frac{d}{dt}\tilde{\rho} = & - \sum_{n,j} \int_0^t d\tau [\sigma_j^- \sigma_j^+ \rho(t) e^{-i(\omega_j - \omega_{n,j})\tau} |g_{n,j}|^2 n(\omega_{n,j}, T_j) \\
& - \sigma_j^+ \rho(t) \sigma_j^- e^{-i(\omega_j - \omega_{n,j})\tau} |g_{n,j}|^2 n(\omega_{n,j}, T_j) \\
& + \rho(t) \sigma_j^+ \sigma_j^- e^{-i(\omega_j - \omega_{n,j})\tau} |g_{n,j}|^2 (n(\omega_{n,j}, T_j) + 1) \\
& - \sigma_j^- \rho(t) \sigma_j^+ e^{-i(\omega_j - \omega_{n,j})\tau} |g_{n,j}|^2 (n(\omega_{n,j}, T_j) + 1) \\
& + \sigma_j^+ \sigma_j^- \rho(t) e^{i(\omega_j - \omega_{n,j})\tau} |g_{n,j}|^2 (n(\omega_{n,j}, T_j) + 1) \\
& - \sigma_j^- \rho(t) \sigma_j^+ e^{i(\omega_j - \omega_{n,j})\tau} |g_{n,j}|^2 (n(\omega_{n,j}, T_j) + 1) \\
& + \rho(t) \sigma_j^- \sigma_j^+ e^{i(\omega_j - \omega_{n,j})\tau} |g_{n,j}|^2 n(\omega_{n,j}, T_j) \\
& - \sigma_j^+ \rho(t) \sigma_j^- e^{i(\omega_j - \omega_{n,j})\tau} |g_{n,j}|^2 n(\omega_{n,j}, T_j)].
\end{aligned} \tag{3.2}$$

After carrying out the integrations as in the strong interaction case, the expression becomes

$$\begin{aligned}
\frac{d}{dt}\tilde{\rho} = & - \sum_{j=1}^2 [(\pi J_j(\omega_j) n(\omega_j, T_j) + iP \int_0^\infty d\omega' \frac{J_j(\omega')}{\omega' - \omega_j}) n(\omega_j, T_j) \sigma_j^- \sigma_j^+ \rho(t) \\
& - (\pi J_j(\omega_j) n(\omega_j, T_j) + iP \int_0^\infty d\omega' \frac{J_j(\omega')}{\omega' - \omega_j}) n(\omega_j, T_j) \sigma_j^+ \rho(t) \sigma_j^- \\
& + (\pi J_j(\omega_j) (n(\omega_j, T_j) + 1) + iP \int_0^\infty d\omega' \frac{J_j(\omega')}{\omega' - \omega_j}) (n(\omega_j, T_j) + 1) \rho(t) \sigma_j^- \sigma_j^+ \\
& - (\pi J_j(\omega_j) (n(\omega_j, T_j) + 1) + iP \int_0^\infty d\omega' \frac{J_j(\omega')}{\omega' - \omega_j}) (n(\omega_j, T_j) + 1) \sigma_j^- \rho(t) \sigma_j^+ \\
& + (\pi J_j(\omega_j) (n(\omega_j, T_j) + 1) - iP \int_0^\infty d\omega' \frac{J_j(\omega')}{\omega' - \omega_j}) (n(\omega_j, T_j) + 1) \sigma_j^+ \sigma_j^- \rho(t) \\
& - (\pi J_j(\omega_j) (n(\omega_j, T_j) + 1) - iP \int_0^\infty d\omega' \frac{J_j(\omega')}{\omega' - \omega_j}) (n(\omega_j, T_j) + 1) \sigma_j^- \rho(t) \sigma_j^+ \\
& + (\pi J_j(\omega_j) n(\omega_j, T_j) - iP \int_0^\infty d\omega' \frac{J_j(\omega')}{\omega' - \omega_j}) (n(\omega_j, T_j) + 1) \rho(t) \sigma_j^- \sigma_j^+ \\
& - (\pi J_j(\omega_j) n(\omega_j, T_j) - iP \int_0^\infty d\omega' \frac{J_j(\omega')}{\omega' - \omega_j}) (n(\omega_j, T_j) + 1) \sigma_j^+ \rho(t) \sigma_j^-].
\end{aligned} \tag{3.3}$$

Simplification leads to

$$\begin{aligned}
\frac{d}{dt}\tilde{\rho} = & \sum_{j=1}^2 [(2\pi J_j(\omega_j) n(\omega_j, T_j) (\sigma_j^+ \rho(t) \sigma_j^- - \frac{1}{2} \{\sigma_j^- \sigma_j^+, \rho(t)\})_+) \\
& + (2\pi J_j(\omega_j) (n(\omega_j, T_j) + 1) (\sigma_j^- \rho(t) \sigma_j^+ - \frac{1}{2} \{\sigma_j^+ \sigma_j^-, \rho(t)\})_+)
\end{aligned}$$

$$-iP \int_0^\infty d\omega' \frac{J_j(\omega')}{\omega' - \omega_j} n(\omega_j, T_j) [\sigma_j^- \sigma_j^+, \rho(t)] - iP \int_0^\infty d\omega' \frac{J_j(\omega')}{\omega' - \omega_j} (n(\omega_j, T_j) + 1) [\sigma_j^+ \sigma_j^-, \rho(t)]. \quad (3.4)$$

The first two terms on the right hand side of (3.4) constitute the Dissipator $D(\rho)$. The last two terms which represent Lamb shift effects are again neglected [5]. Finally, the equation is transformed back to the Schrödinger picture using the relation

$$\dot{\rho} = -i[H_S, \rho] + D(\rho). \quad (3.5)$$

3.1 Two Weakly Interacting Spins

In this particular case, two weakly interacting spins are each coupled to two separate baths at different temperatures. The Hamiltonian of the system is taken as

$$\hat{H}_S = \frac{\epsilon_1}{2} \hat{\sigma}_1^z + \frac{\epsilon_2}{2} \hat{\sigma}_2^z + K(\hat{\sigma}_1^+ \hat{\sigma}_2^- + \hat{\sigma}_1^- \hat{\sigma}_2^+). \quad (3.6)$$

The equation of motion is given by (3.5). The solution for the diagonal elements and the two non-diagonal elements can be written as

$$\frac{d}{dt} \begin{pmatrix} \rho_{11}(t) \\ \rho_{22}(t) \\ \rho_{23}(t) \\ \rho_{32}(t) \\ \rho_{33}(t) \\ \rho_{44}(t) \end{pmatrix} = M_{ij} \begin{pmatrix} \rho_{11}(t) \\ \rho_{22}(t) \\ \rho_{23}(t) \\ \rho_{32}(t) \\ \rho_{33}(t) \\ \rho_{44}(t) \end{pmatrix}. \quad (3.7)$$

The non-zero components of the 6×6 matrix M_{ij} are:

$$M_{11} = -2\pi J_1(\omega_1)(n(T_1, \omega_1) + 1) - 2\pi J_2(\omega_2)(n(T_2, \omega_2) + 1),$$

$$M_{12} = 2\pi J_2(\omega_2)n(T_2, \omega_2),$$

$$M_{15} = 2\pi J_1(\omega_1)n(T_1, \omega_1),$$

$$M_{21} = 2\pi J_2(\omega_2)(n(T_2, \omega_2) + 1),$$

$$\begin{aligned}
M_{22} &= -2\pi J_1(\omega_1)(n(T_1, \omega_1) + 1) - 2\pi J_2(\omega_2)n(T_2, \omega_2), \\
M_{23} &= iK, \\
M_{24} &= -iK, \\
M_{26} &= 2\pi J_1(\omega_1)n(T_1, \omega_1), \\
M_{32} &= iK, \\
M_{33} &= -\frac{1}{2}[2\pi J_1(\omega_1)(n(T_1, \omega_1) + 1) \\
&+ 2\pi J_2(\omega_2)(n(T_2, \omega_2) + 1) + 2\pi J_1(\omega_1)n(T_1, \omega_1) + 2\pi J_2(\omega_2)n(T_2, \omega_2)] - i(\Lambda_2 - \Lambda_3), \\
M_{35} &= -iK, \\
M_{42} &= -iK, \\
M_{44} &= -\frac{1}{2}[2\pi J_1(\omega_1)(n(T_1, \omega_1) + 1) \\
&+ 2\pi J_2(\omega_2)(n(T_2, \omega_2) + 1) + 2\pi J_1(\omega_1)n(T_1, \omega_1) + 2\pi J_2(\omega_2)n(T_2, \omega_2)] + i(\Lambda_2 - \Lambda_3), \\
M_{45} &= iK, \\
M_{51} &= 2\pi J_1(\omega_1)n(T_1, \omega_1), \\
M_{53} &= -iK, \\
M_{42} &= iK, \\
M_{55} &= -2\pi J_2(\omega_2)(n(T_2, \omega_2) + 1) - 2\pi J_1(\omega_1)n(T_1, \omega_1), \\
M_{56} &= 2\pi J_2(\omega_2)(n(T_2, \omega_2) + 1), \\
M_{62} &= 2\pi J_1(\omega_1)n(T_1, \omega_1), \\
M_{65} &= 2\pi J_2(\omega_2)n(T_2, \omega_2), \\
M_{66} &= -2\pi J_1(\omega_1)n(T_1, \omega_1) - 2\pi J_2(\omega_2)n(T_2, \omega_2),
\end{aligned}$$

where

$$\Lambda_2 = -\Lambda_3 = \frac{\epsilon_1 - \epsilon_2}{2}.$$

For the weakly interacting spins, the steady state is considered. To find the solution, it is noted that in this state,

$$\frac{d}{dt} \begin{pmatrix} \rho_{11}(t) \\ \rho_{22}(t) \\ \rho_{23}(t) \\ \rho_{32}(t) \\ \rho_{33}(t) \\ \rho_{44}(t) \end{pmatrix} = 0.$$

A vector \vec{X} is found such that $M\vec{X} = 0$ where M is the matrix in (3.5). The elements of \vec{X} are the diagonal elements of the steady state density matrix and the two non-vanishing elements ρ_{23} and ρ_{32} . In order to preserve probability, the diagonal elements are normalized. For the particular case where $\epsilon_1 = \epsilon_2$ in the Hamiltonian (3.6), the solved density matrix has the following non-vanishing components:

$$\rho_{11} = \frac{4K^2\chi_2^2 + \chi_2^-\chi_2^+(\chi_1 + \chi_2)^2}{(\chi_1 + \chi_2)^2(4K^2 + (\chi_1^- + \chi_2^-)(\chi_1^+ + \chi_2^+))},$$

$$\rho_{22} = \rho_{33} = \frac{4K^2\chi_1\chi_2 + \chi_1^+\chi_2^-(\chi_1 + \chi_2)^2}{(\chi_1 + \chi_2)^2(4K^2 + (\chi_1^- + \chi_2^-)(\chi_1^+ + \chi_2^+))},$$

$$\rho_{23} = \rho_{32}^* = \frac{i2K(\chi_1^-\chi_2^+ - \chi_1^+\chi_2^-)}{(\chi_1 + \chi_2)^2(4K^2 + (\chi_1^- + \chi_2^-)(\chi_1^+ + \chi_2^+))},$$

$$\rho_{44} = 1 - (\rho_{11} + \rho_{22} + \rho_{33}).$$

In the above expressions, the following abbreviations have been used:

$$\chi_1 = \chi_1^- + \chi_1^+,$$

$$\chi_2 = \chi_2^- + \chi_2^+,$$

$$\chi_1^- = J_1(\omega_1)(n(T_1, \omega_1) + 1),$$

$$\chi_1^+ = J_2(\omega_2)(n(T_2, \omega_2) + 1),$$

$$\chi_2^- = J_1(\omega_1)n(T_1, \omega_1),$$

$$\chi_2^- = J_2(\omega_2)n(T_2, \omega_2).$$

With the solution for the density matrix obtained, the entanglement dynamics of the system can be studied using the entanglement as a measure.

Chapter 4

Results

4.1 Non-steady State

In this chapter, the results of the analytical study of the interaction models are presented. The quantity of interest in all cases is the entanglement between the spins. Using the concurrence as the measure, the variation of the entanglement with the parameters of time and temperature is demonstrated. For both the strong spin-spin interaction model and the weak spin-spin interaction model, the environmental spectral density that is used is the Lorentzian distribution (2.9). Two situations are considered. In the first situation, i.e. the non-steady state, the entanglement of any system varies with time for given parameters such as temperature. This allows for comparisons of the concurrence-time relations to be made between different initial states for each set of parameters. In this thesis, this is done only for the strong spin-spin interaction model. In the second situation, i.e. the steady state, time is no longer a factor as the concurrence reaches a constant value. Here, the concurrence-temperature relations are studied for both the strong spin-spin interaction model and the weak spin-spin interaction model and comparisons are made between them.

We start by analyzing the entanglement for the initial two-spin state $|\psi\rangle = \frac{1}{\sqrt{2}}(|10\rangle + |01\rangle)$. Figure 4.1 demonstrates how the concurrence varies with time for the chosen parameters. The concurrence is shown for different bath temperatures. The concurrence is seen to be maximum

at the initial time. It then begins to decrease as time passes. It is clear from the figure that an increase in the bath temperature results in rapid destruction of the entanglement. The entanglement is seen to fall to a particular constant value that is dependent on the bath temperatures, T_1 and T_2 . Figures 4.2 and 4.3 respectively shown the concurrence for the initial two-spin states $|\psi\rangle = |10\rangle$ and $|\psi\rangle = |11\rangle$. Here, the concurrence rises to a maximum value that then remains constant.

Figure 4.4, shows how the entanglement varies with time for the initial two-spin states $\psi = \frac{1}{\sqrt{2}}(|10\rangle + |01\rangle)$, $\psi = |10\rangle$ and $\psi = |11\rangle$. All the systems have the same bath temperature for comparison purposes. It is seen that after initial variations, the concurrence flattens to the same value for all the states. This is the result that was predicted theoretically as all the non-diagonal elements of the density matrix vanish and the diagonal elements become constants, independent of time.

Similar results are obtained when three-spin systems are considered. Figure 4.5 shows how the entanglement is dependent on bath temperatures for the initial state $\frac{1}{\sqrt{3}}(|100\rangle + |010\rangle + |001\rangle)$. Like for the two spins system, Figure 4.6 shows how different initial states all end up with the same value for the concurrence after a sufficiently long enough time. Once again, this is a manifestation of the fact that all the non-diagonal elements vanish and the diagonal elements become independent of time.

Figure 4.6 also shows another phenomenon that is not so apparent in the two spins systems but is clearly evident for the three spins system. It is the observation that the form of the curve of the variation of the concurrence with time also depends on whether the initial state is symmetric, like $|111\rangle$, or non-symmetric, like $|100\rangle$ and $\frac{1}{\sqrt{2}}(|100\rangle + |010\rangle + |001\rangle)$. For symmetric states, the entanglement builds to the constant value without any oscillations. For non-symmetric states, oscillations occur before the constant value is reached. This is just a reflection of the fact that for the non-symmetric states, the qubits point in different direction to begin with and so an energy exchanges take place between them before the steady state is reached.

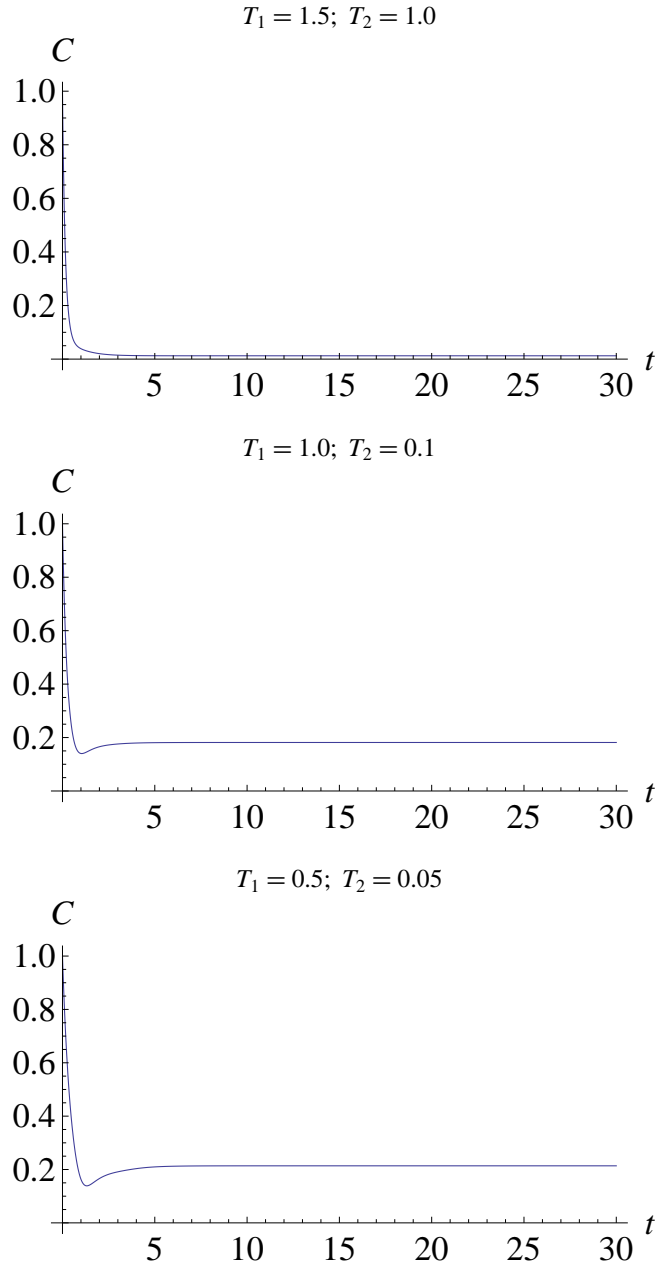


Figure 4.1: The variation of the concurrence with time for the strong spin-spin interaction model when the initial state is $|\psi\rangle = \frac{1}{\sqrt{2}}(|10\rangle + |01\rangle)$. The bath temperatures T_1 and T_2 are shown for each of the curves. The chosen Hamiltonian parameters are $\epsilon_1 = 2, \epsilon_2 = 1, K = 1$. The decrease in the concurrence with increasing temperature is obvious.

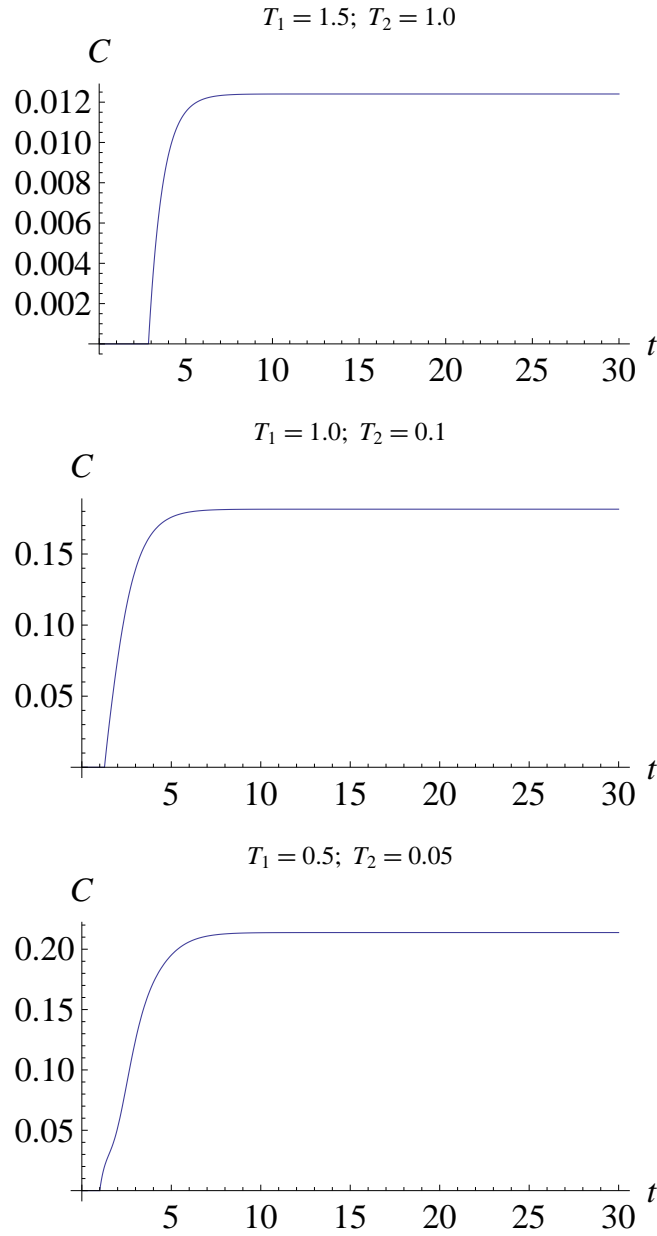


Figure 4.2: The variation of the concurrence with time for the initial two-spin state $|\psi\rangle = |10\rangle$. In this case $\epsilon_1 = 2, \epsilon_2 = 1, K = 1$. The concurrence is seen to increase to a constant value.

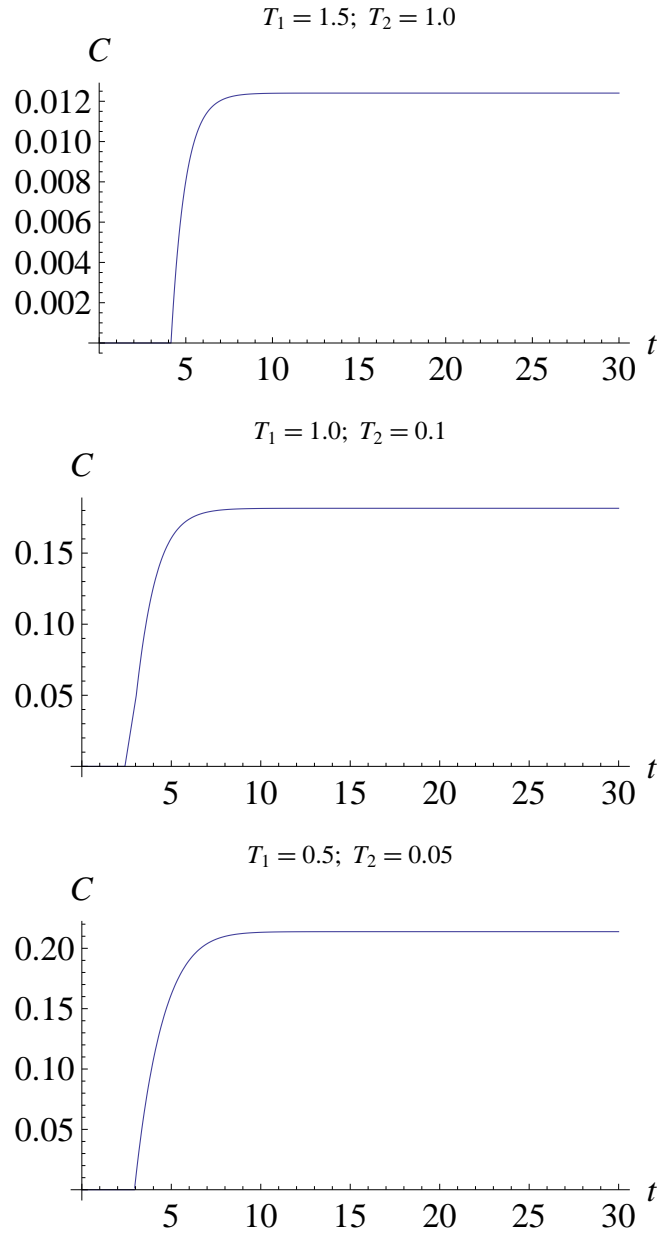


Figure 4.3: The variation of the concurrence with time for the initial two-spin state $|\psi\rangle = |11\rangle$. The Hamiltonian parameters are $\epsilon_1 = 2, \epsilon_2 = 1, K = 1$. Initially, the system is not entangled. Entanglement then builds with time to a constant level.

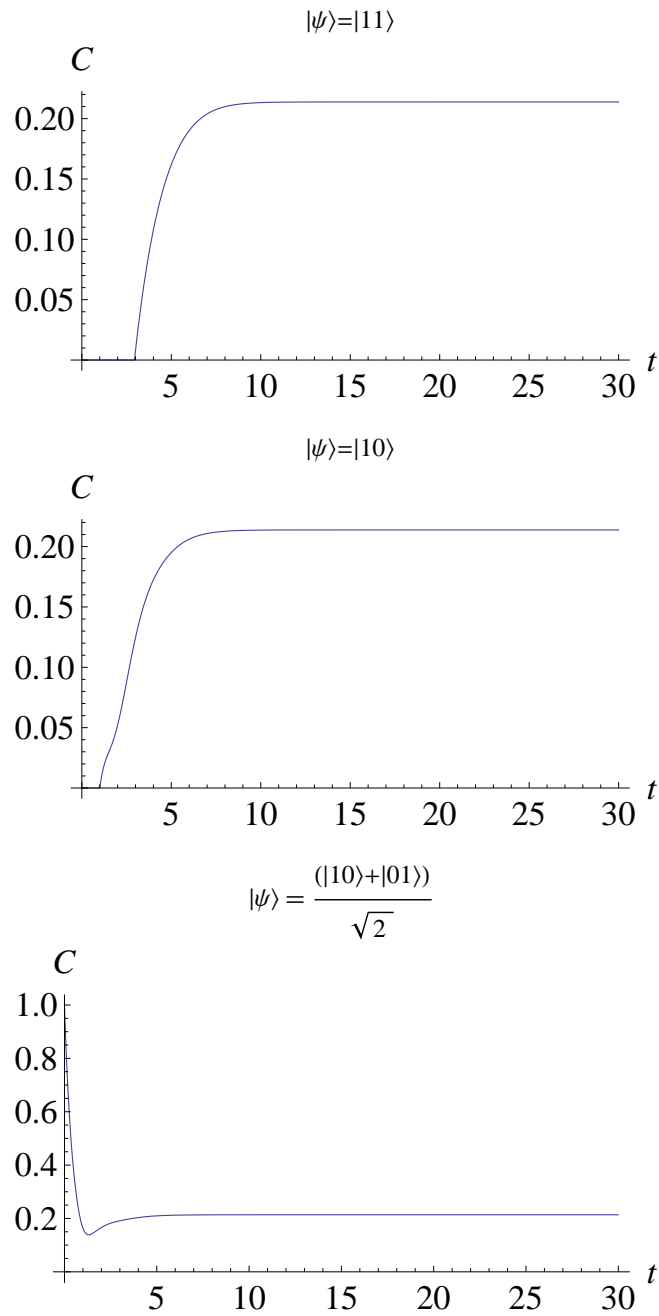


Figure 4.4: Concurrence vs. time for different initial two spin states. The temperatures for each state are $T_1 = 0.5$, $T_2 = 0.01$, and the Hamiltonian parameters are $\epsilon_1 = 2$, $\epsilon_2 = 1$ and, $K = 1$. All the different states are seen to end up with the same value for the concurrence.

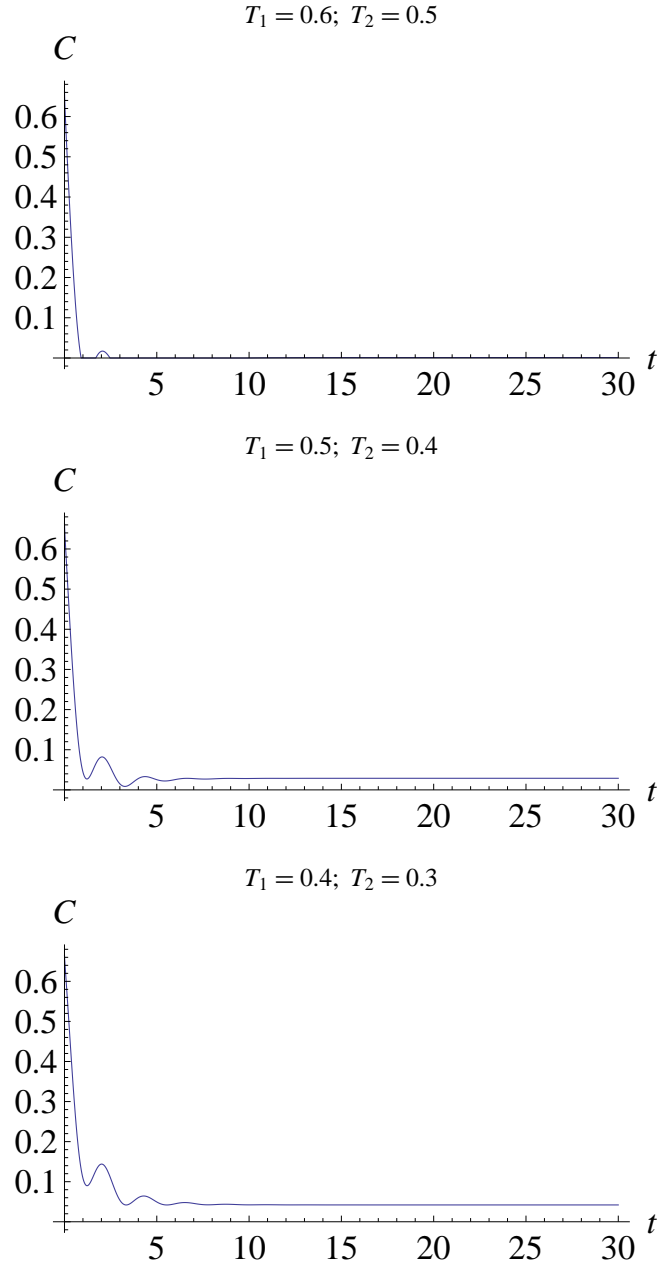


Figure 4.5: The variation of the concurrence with time for the initial three-spin state $\psi = \frac{1}{\sqrt{3}}(|100\rangle + |010\rangle + |001\rangle)$. The bath temperatures are shown for each case. Here $\epsilon_1 = 2, \epsilon_2 = 1, K = 1$

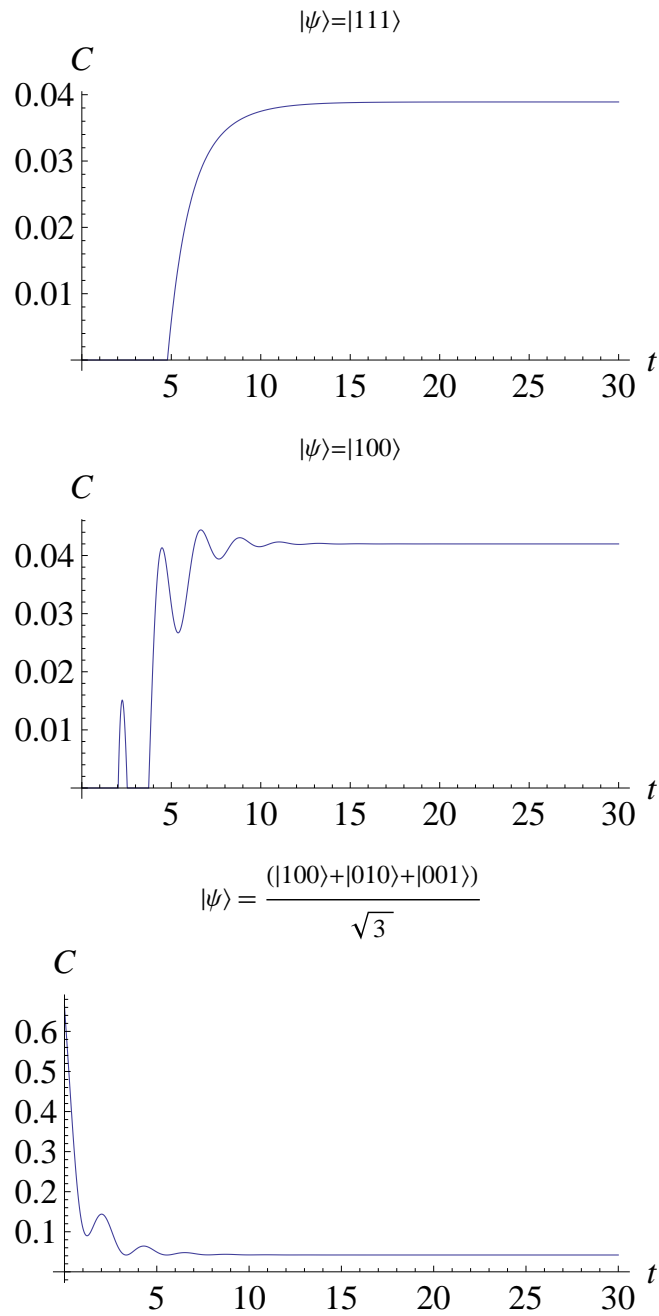


Figure 4.6: Concurrence vs. time for the indicated three-spin initial states . The temperatures are $T_1 = 0.4, T_2 = 0.3$, and the Hamiltonian parameters are $\epsilon_1 = 2, \epsilon_2 = 1, K = 1$. As in the two spins case, entanglement for all the states converges to the same value.

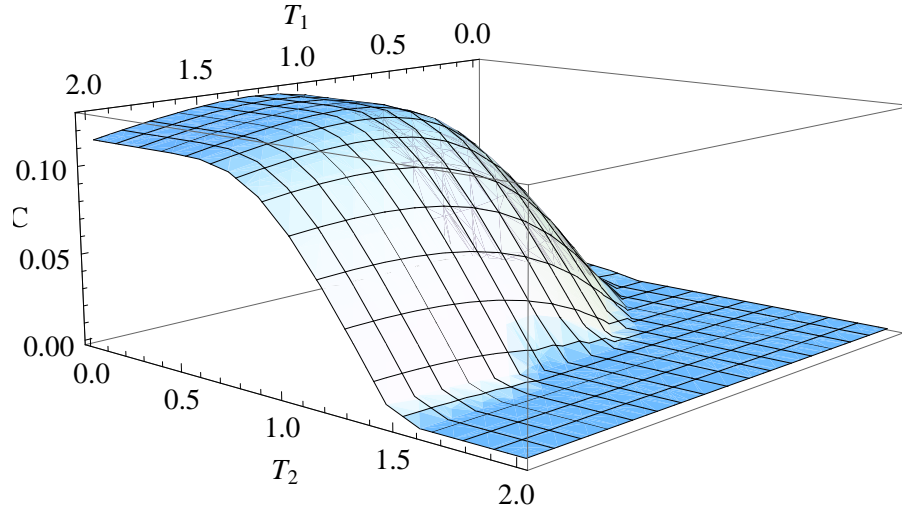


Figure 4.7: A surface-plot of the Concurrence as a function of the bath temperatures for the strong two spins interaction system. This is for the two-spin steady state case where $\epsilon_1 = 5, \epsilon_2 = 1, K = 1$. The decrease of entanglement with increasing temperature is apparent.

4.2 Steady State

As has been shown analytically, in the limit, as $t \rightarrow \infty$, all the diagonal elements of ρ vanish. The diagonal elements become dependent only on the bath temperatures T_1 and T_2 .

Given that in the steady state time no longer affects the entanglement, the effects of the bath temperatures on the concurrence can now be studied. The steady state also provides the opportunity for comparisons to be made between entanglement in the strong spin-spin interaction model and the weak spin-spin interaction model.

Figure 4.7 is a surface-plot of the variation of the concurrence with the bath temperatures for the two spins system. It is observed that the increase in either bath temperature results in a steady fall in the concurrence. At high enough temperatures, the concurrence drops to zero. These results are, as would be expected, the same for both the two spins system and the three spins system. When a comparison is made with the weak spin interaction system, it is seen that for the same parameters of temperature and energy, the concurrence for the weak spin system is much lower. In fact, in the weak interaction system, the entanglement is zero for the most part in the case of the parameters that are given in the Figures 4.7 and 4.8.

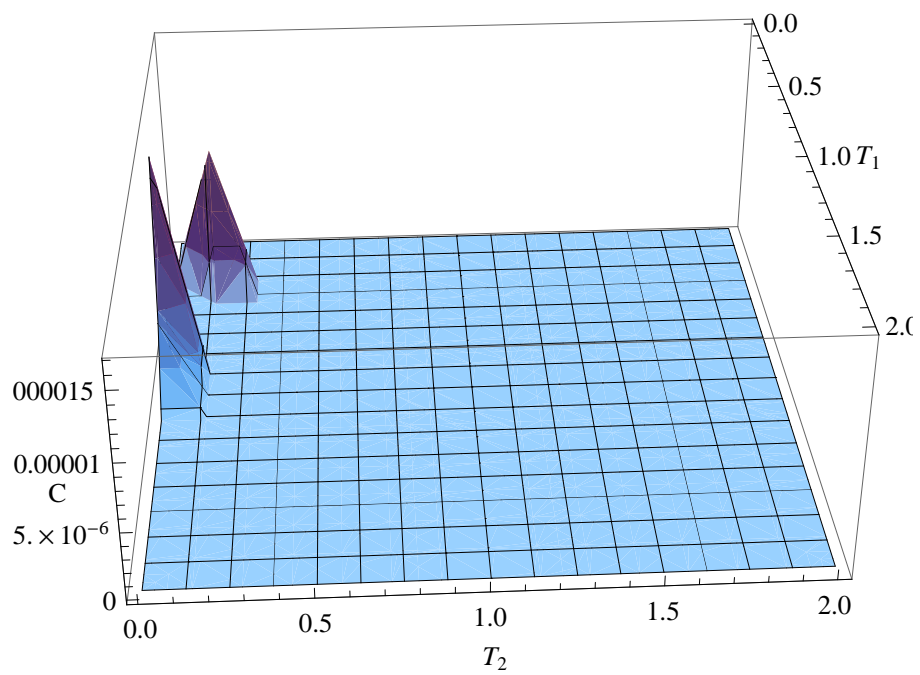


Figure 4.8: A surface-plot of the Concurrence as a function the bath temperatures for the weak two spins interaction system. In this case $\epsilon_1 = 5$, $\epsilon_1 = 1$, $K = 0.01$

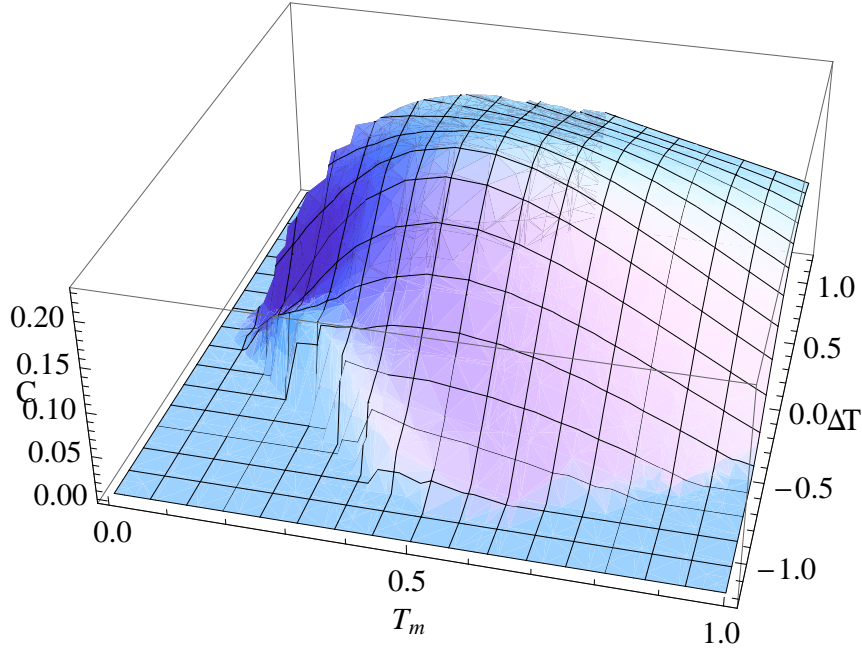


Figure 4.9: A surface-plot of the Concurrence as a function of the temperature difference between the two baths ΔT and the mean temperature T_m for the strong two spins interaction system. The chosen parameters are $\epsilon_1 = 5, \epsilon_2 = 1, K = 1$

The steady state also provides an opportunity to see how the entanglement is affected by both the mean bath temperature, $T_m = (T_1 + T_2)/2$ and the temperature difference between the baths $\Delta T = T_1 - T_2$. Figures 4.9 and 4.10 show the results for the strong and weak spin interaction systems respectively.

It is observed that an increase in T_m has the effect of reducing the value of the concurrence. Comparison of the figures 4.9 and 4.10 reveals a difference between the strong spin-spin interaction model and the weak spin-spin interaction model. Generally, for any given values of the bath temperatures, the entanglement for the weak spin interaction is much lower than for the strong interaction. The figures also reveals that for the strong interaction model, the concurrence is maximum when ΔT is zero. This is not the case for the weak interaction model, where the maximum value is not necessarily at $\Delta T = 0$.

One of the clearest results that emerged from our study is the relationship between the bath temperature and the concurrence. For the strong spin-spin interaction model, it is seen that

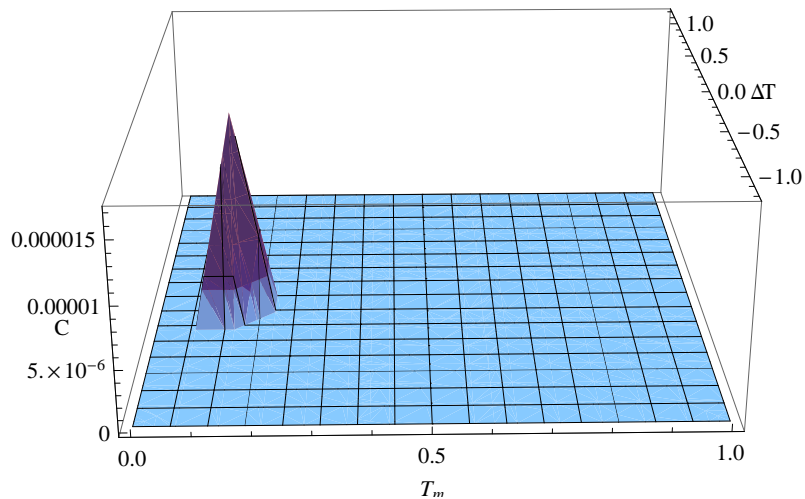


Figure 4.10: A surface-plot of the Concurrence as a function of the temperature difference between the two baths ΔT and the mean temperature T_m for the weak two spins interaction system. The parameters are $\epsilon_1 = 5$, $\epsilon_2 = 1$, $K = 0.01$.

an increase in temperature from very low values reduces the concurrence. At high enough temperatures, the concurrence vanishes all together. This is true for both the two-spins and the three-spins cases. We have also observed how in the strong interaction case, all systems, regardless of the initial conditions, end up with the same amount of entanglement for given sets of parameters.

There are some obvious differences between the steady state dynamics for the strong interaction model and for the weak interaction model. In the strong interaction case, all the non-diagonal elements of the density matrix vanish. In the weak interaction case, some do not vanish. The dependence of the concurrence on temperature is different for these two models. In the strong interaction case, there is a wide range of temperatures over which the concurrence is not zero. The weak interaction case, on the other hand provides only a very narrow range of temperatures over which any entanglement is observed.

Chapter 5

Conclusion

This thesis has been focused on the study of the dynamics of the thermal entanglement of spin chains. In the first part of the thesis, we highlighted some of the many possible applications of entanglement. In quantum information and quantum computing, the basic unit of information is the qubit, which can be represented by a superposition of spin states. Efficient storage, manipulation and retrieval of information can only be possible if the dynamics of the entanglement between the qubits is understood. In quantum teleportation, it is the entanglement between the separated parts of a pair of qubits that allows for exact copies of another qubit to be teleported. In quantum cryptography, entanglement enables information transmission between parties to be made securely.

Transition from the theoretical to the practical means that all the quantum systems of interest would have to be exposed to the environment. The non-unitary evolution of these open systems is much more complicated than the unitary evolution of closed systems. The derivation of the master equation for the analysis of the dynamics of open systems in the Born-Markov approximation has been demonstrated. Two models have been considered; the strong spin-spin interaction model and the weak spin-spin interaction model. For each of these models the appropriate equation which describes the evolution of the system with time has been given and solved. From these solutions, the dynamics of the entanglement of the systems have been studied using analytical methods. This has been done with the concurrence as the measure of

the entanglement.

One of the objectives of the study has been to see what the effects of bath temperatures are on the entanglement of the systems. Of the results obtained, one of the most obvious has been the fact that the entanglement of the systems decreases with increasing bath temperature. As expected, this result was obtained for all the states and for both the strong and the weak spin-spin interaction models.

Observations also verified a result that was obtained in the study of the solutions of systems. It was shown analytically that in the limit of large times, the density matrix reduces to one where the diagonal elements are the only non-zero elements. This was shown by the result that given the same bath temperatures all the states show the same value of the concurrence.

In this steady state, it has been possible to observe how the concurrence varies with both the mean temperature T_m and the bath temperature difference ΔT for both models. For all temperatures, the entanglement in the weak spin interaction model has been shown to be considerably less than it is for the strong interaction model. Indeed, it is only for a very narrow range of temperature that the concurrence is above zero.

The other notable difference is that for the strong spin-spin interaction model, the highest value for the concurrence occurs when the difference between the bath temperatures $\Delta T = 0$. This is not seen to be the case for the weak spin-spin interaction model.

The analytical methods used in this thesis can be used to extend this study. It would be useful to see how the entanglement-temperature variation patterns are affected as the number of spins being considered increases to four or more spins. Comparisons can then be made between the two models.

Some approximations and simplifications were made in this thesis. An important step that was taken was the use of the Markovian approximation. A possible area of further study is the comparison of the weak and strong interaction models with the use of master equations obtained using non-Markovian considerations.

In the study of the three-spin system, the analysis was simplified by assuming that all the spins had the same energy value. The situation obviously becomes a lot more complicated when

different energy values are assigned to different spins. Studies can be done to see how this would affect the entanglement between those spins, and how that in turn would be affected by the bath temperatures.

Appendix

Sets Of Linked Density Matrix Elements

The following eight sets of elements are those of the reduced density matrix for the three-spin system. They are linked in a way that is similar to the elements in Section 2.4. Listed for each set are the matrices and the corresponding eigenvalues, and in a manner equivalent to that used in Section 2.4, it can be shown that at large times these non-diagonal elements vanish.

i. For the density matrix elements $\rho_{15}, \rho_{26}, \rho_{73}, \rho_{84}$, the matrices and corresponding eigenvalues used in the proof are:

$$\Delta_3 = -\frac{1}{2}(Z^+ + Z^-) + i\epsilon,$$

$$M_3 = \begin{pmatrix} -(X^- + Y^-) & F^+ & G^+ & 0 \\ F^- & -(X^+ + Y^-) & 0 & G^+ \\ G^- & 0 & -(Y^+ + X^-) & F^+ \\ 0 & G^- & F^- & -(X^+ + Y^+) \end{pmatrix}.$$

$$\lambda_i = -\frac{1}{2}(X + Y) \pm \sqrt{X_F^2 + Y_G^2 \pm 2X_F Y_G}$$

$$= -\frac{1}{2} \left(X + Y \pm \sqrt{(X_F \pm Y_G)^2} \right),$$

where

$$X_F = \sqrt{(X^+ - X^-)^2 + 4F^+ F^-}$$

and

$$Y_G = \sqrt{(Y^+ - Y^-)^2 + 4G^+ G^-}.$$

ii. For the density matrix elements ρ_{13}, ρ_{24} , the matrices and corresponding eigenvalues are:

$$\Delta_4 = -\frac{1}{2}(Y^- + Z^+ + Y^+ + Z^-) + 2i\epsilon,$$

$$M_4 = \begin{pmatrix} -X^- & -X^+ \\ -X^- & -X^+ \end{pmatrix}.$$

$$\lambda_i = 0, -(X^- + X^+).$$

iii. For ρ_{16}, ρ_{74} , the matrices and corresponding eigenvalues are:

$$\Delta_5 = -\frac{1}{2}(X^+ + Z^+ + X^- + Z^-) - i(2\epsilon - \sqrt{2}K),$$

$$M_4 = \begin{pmatrix} -Y^- & -Y^+ \\ -Y^- & -Y^+ \end{pmatrix}.$$

$$\lambda_i = 0, -(Y^- + Y^+).$$

iv. For $\rho_{17}, \rho_{28}, \rho_{53}, \rho_{64}$, the matrices and corresponding eigenvalues are:

$$\Delta_6 = -\frac{1}{2}(Y^+ + Y^-) + i(\epsilon - \sqrt{2}K),$$

$$M_6 = \begin{pmatrix} -(X^- + Z^-) & -F^+ & -H^+ & 0 \\ -F^- & -(X^+ + Z^-) & 0 & -H^+ \\ -H^- & 0 & -(Z^+ + X^-) & -F^+ \\ 0 & H^- & -F^- & -(X^+ + Z^+) \end{pmatrix}.$$

$$\begin{aligned} \lambda_i &= -\frac{1}{2}(X + Z) \pm \sqrt{X_F^2 + Z_H^2 \pm 2X_F Z_H} \\ &= -\frac{1}{2} \left(X + Z \pm \sqrt{(X_F \pm Z_H)^2} \right). \end{aligned}$$

$$X_F = \sqrt{(X^+ - X^-)^2 + 4F^+ F^-},$$

$$Z_H = \sqrt{(Z^+ - Z^-)^2 + 4H^+H^-}.$$

v. For ρ_{18}, ρ_{54} , the matrices and corresponding eigenvalues are:

$$\Delta_7 = -\frac{1}{2}(X^- + Y^+ + X^+ + Y^-) + i2\epsilon + \sqrt{2}K,$$

$$M_7 = \begin{pmatrix} -Z^- & Z^+ \\ Z^- & -Z^+ \end{pmatrix}.$$

$$\lambda_i = 0, -(Z^- + Z^+).$$

vi. For ρ_{25}, ρ_{83} , the matrices and corresponding eigenvalues are:

$$\Delta_8 = -\frac{1}{2}(X^+ + Z^+ + X^- + Z^-) + i2K,$$

$$M_8 = \begin{pmatrix} -Y^- & Y^+ \\ Y^- & -Y^+ \end{pmatrix}.$$

$$\lambda_i = 0, -(Y^- + Y^+).$$

vii. For ρ_{27}, ρ_{63} , the matrices and corresponding eigenvalues are:

$$\Delta_9 = -\frac{1}{2}(X^+ + Y^+ + X^- + Y^-) + i\sqrt{2}K,$$

$$M_9 = \begin{pmatrix} -Z^- & Z^+ \\ Z^- & -Z^+ \end{pmatrix}.$$

$$\lambda_i = 0, -(Z^- + Z^+).$$

viii. For ρ_{57}, ρ_{68} , the matrices and corresponding eigenvalues are:

$$\Delta_{10} = -\frac{1}{2}(Y^+ + Z^+ + Y^- + Z^-) + i2\sqrt{2}K,$$

$$M_{10} = \begin{pmatrix} -Z^- & Z^+ \\ Z^- & -Z^+ \end{pmatrix}.$$

$$\lambda_i = 0, -(Z^- + Z^+).$$

The hermiticity of the density matrix means that $\lim_{t \rightarrow \infty} \rho_{ij}(t) = \lim_{t \rightarrow \infty} \rho_{ji}(t)$. Thus, the density matrix elements that have been considered above and in Chapter 2 are all that are needed to prove that all the non-diagonal elements vanish at large times.

Bibliography

- [1] W. Greiner, *Quantum Mechanics An Introduction* (Springer, Berlin, 1994).
- [2] C. Cohen-Tannoudji, B. Diu, F. Lalöe, *Quantum Mechanics* (John Wiley and Sons , London, 1977).
- [3] R. L. Liboff, *Introductory Quantum Mechanics* (Addison-Wesley, New York, 1993).
- [4] A. S. Davydov, *Quantum Mechanics* (Pergamon Press, London, 1965).
- [5] H. P. Breuer and F. Petruccione, *The Theory of Open Quantum Systems* (Oxford University Press, Oxford, 2002).
- [6] A. Einstein, B. Podolsky, N. Rosen, *Phys. Rev.* **47**, 777 (1935).
- [7] A. Aspect, P. Grangier, G. Roger, *Phys. Rev. Lett.* **49**, 91 (1982).
- [8] M. Nielsen and I. Chuang, *Quantum Computation and Quantum Information* (Cambridge University Press, Cambridge, 2000).
- [9] C. H. Bennett and D. P. DiVincenzo, *Nature (London)* **404**, 247 (2000).
- [10] C. H. Bennett and G. Brassard, *Proceedings of IEEE International Conference on Computers, Systems, and Signal Processing (IEEE, 1984)*, page 175.
- [11] A. K. Ekert, *Phys. Rev. Lett.* **67**, 661 (1991).
- [12] C. H. Bennett, G. Brassard, C. Crepeau, R. Jozsa, A. Peres. W. K. Wothers, *Phys. Rev. Lett.* **70**, 1895 (1993).

- [13] D. Bouwmeester, Jian-Wei Pan, K. Mattle, M. Eibl, H. Weinfurter, A. Zeilinger, *Nature* (London) **390**, 575 (1997).
- [14] M. C. Arnesen, S. Bose, V. Vedral, *Phys. Rev. Lett.* **87**, 017901 (2001).
- [15] X. L. Huang, J. L. Guo, X. X. Yi, *Phys. Rev. A* **80**, 054301 (2009).
- [16] P. A. M. Dirac, *The Principles Of Quantum Mechanics, Fourth Edition* (Oxford University Press, Oxford, 1958).
- [17] H. Carmichael, *An Open Systems Approach to Quantum Optics* (Springer-Verlag, London, 1993).
- [18] C. W. Gardiner, P. Zoller, *Quantum Noise - A Handbook of Markovian and Non-Markovian Quantum Stochastic Methods with Application to Quantum Optics* (Springer-Verlag, Berlin, 1991).
- [19] Tzu-Chieh Wei, K. Nemoto, P. M. Goldbart, P. G. Kwiat, W. J. Munro, F. Verstraete, *Phys. Rev. A* **67**, 022110 (2003).
- [20] K. Zyczkowski, P. Horodecki, A. Sanpera, and M. Lewenstein, *Phys. Rev. A* **58**, 883 (1998).
- [21] G. Vidal and R. F. Werner, *Phys. Rev. A* **65**, 032314 (2002).
- [22] W. K. Wootters, *Phys. Rev. Lett.* **80**, 2245 (1998).
- [23] I. Sinaysky, F. Petruccione, D. Burgarth, *Phys. Rev. A* **78**, 062301 (2008).
- [24] M. Reed and B. Simon, *Methods of Modern Mathematical Physics* (Academic Press Press, New York, 1980).